NATIONAL ADVISORY COMMITTEE FOR AERONAUTICS

TECHNICAL NOTE

No. 1539

MEASUREMENTS OF THE PRESSURE DISTRIBUTION ON THE HORIZONTAL-TAIL SURFACE OF A TYPICAL PROPELLER-DRIVEN PURSUIT AIRPLANE IN FLIGHT. III - TAIL LOADS IN ABRUPT PULL-UP PUSH-DOWN MANEUVERS

By Melvin Sadoff and Lawrence A. Clousing

Ames Aeronautical Laboratory
Moffett Field, Calif.

Washington
February 1948

NATIONAL ADVISORY COMMITTEE FOR AERONAUTICS

TECHNICAL NOTE NO. 1539

MEASUREMENTS OF THE PRESSURE DISTRIBUTION ON THE HORIZONTAL-TAIL SURFACE OF A TYPICAL PROPELLER-DRIVEN PURSUIT AIRPLANE IN FLIGHT. III - TAIL LOADS IN ABRUPT PULL-UP PUSH-DOWN MANEUVERS

By Melvin Sadoff and Lawrence A. Clousing

SUMMARY

The total horizontal-tail load and the root bending-moment increments calculated by the use of existing rational procedures are compared with experimental values obtained in pull-up push-down maneuvers on a representative propeller-driven pursuit-type airplane for six different combinations of power, indicated airspeed, and pressure altitude. The computed loads were determined for the experimental elevator motions, and for two estimated linear design motions. There is also presented a comparison between the computed and the experimental load distributions. Briefly touched upon are two abbreviated static methods for predicting the maximum up-loads in pull-up push-down maneuvers.

The results showed that where the computed load and bending-moment increments are determined from measured elevator motions, the agreement with the experimental results is fairly good, thus indicating the validity of methods currently available for calculating maximum maneuvering tail loads. It was also shown that if possible errors in the aerodynamic parameters were accounted for, the agreement between the measured load and bending-moment increments and those computed from the estimated linear elevator motions, for values of maximum airplane load factor approximately the same as those measured, would be practically as good as that obtained using the experimental elevator motions. Results are also included showing that the prediction of the maximum maneuvering loads by the use of two less rigorous abbreviated procedures agreed satisfactorily with the load increments measured. Comparison of the calculated with the experimental load distributions showed that fairly good agreement was obtained when the measured and computed over-all tail loads were in close agreement. However, as compared with experimental results,

an increase in loading was computed for the inboard stabilizer sections and a decrease in loading for the outboard sections. The difference in loading would be equivalent to a root bending moment approximately 10 percent less than the measured values when the overall loads were the same.

INTRODUCTION

In recent years particular emphasis has been placed on providing a simplified rational method for predicting the maneuvering horizontal-tail loads associated with abrupt motions of the elevator. The methods available in the past for computing dynamic tail loads rationally were too unwieldy to use in routine design analyses. Modifications of these methods have been directed primarily toward simplifying and shortening the necessary computations, and toward selection of a longitudinal maneuver which would be amenable to computation and which would adequately define the critical loading condition on the horizontal tail.

In reference 1, for example, general design charts in nondimensional form are given by which the tail-load increment variation in abrupt maneuvers may be determined for any arbitrary elevator motion. Similarly, reference 2, which is a part of the tail-load design requirements for the Army, presents a simple tabular integration method for computing maneuvering tail loads resulting from abrupt linear variations of elevator motion. In this method the time histories of these motions are represented by a series of straight lines simulating a pull-up push-down maneuver for an unstable airplane where the maximum up-elevator deflection is arbitrarily assumed twice the maximum down value.

A check of the validity of the assumptions and mathematical simplifications of references 1 and 2 is, of course, desirable. This is provided in the present investigation by comparing the horizontal-tail load increments measured in flight with values computed for maneuvers having elevator motions identical to the experimental. The computations of tail load for the purpose of this comparison were made using only the method of reference 1, since it is mathematically similar to that of reference 2, and a check of either method would establish the validity of the other. Furthermore, the graphical method of reference 1 is adaptable to the irregular or nonlinear elevator motions that generally occur in flight, which is not the case for the method of reference 2. Some results of comparisons of this type have already been presented in reference 3.

Since designers must use estimated elevator motions in tail-load computations, it is also desirable to determine how closely horizontal-tail-load values computed in linearized pull-up push-down maneuvers

of the type described in reference 2 compare with those measured in pull-up push-down maneuvers made by a pilot in flight. Comparisons are therefore made of the horizontal-tail-load increments measured in flight and those computed by the method of reference 2. In these comparisons the values of elevator deflection used in the computations were taken such that the computed increments of maximum acceleration were identical with those measured in the maneuvers for which the comparisons were made. In setting up rates of elevator motion in these computations, data presented in reference 4 were of considerable value.

Although the methods of references 1 and 2 for computing dynamic tail loads are less unwieldy than the unsimplified classical methods available formerly, considerable computational time is still required in their application. Therefore, information relative to means for shortening the computations is believed of interest. Two abbreviated methods of tail-load computation, which result from modifications of the method of reference 2, are described, and comparisons are made of tail loads computed by these shortened methods with those measured. The comparisons are made on the basis of identical increments of acceleration.

An additional objective of this report is the investigation of the validity of methods currently used for predicting the maneuvering load distributions over the horizontal tail, and information on this subject is presented.

The experimental tail loads and tail-load distributions presented in this note were measured in abrupt pull-up push-down maneuvers for six different combinations of power, indicated airspeed, and pressure altitude. The two previous notes in this series have dealt with tail loads in steady unaccelerated and steady accelerated flight (reference 5), and tail loads in steady sideslips (reference 6).

SYMBOLS

W	airplane weight during test run, pounds
g	acceleration of gravity, feet per second per second
m	airplane mass (W/g), slugs
S	horizontal surface area, square feet
b	horizontal surface span, feet
$\bar{c}$	wing mean aerodynamic chord, feet

c	local tail chord, feet
K_Y	radius of gyration about Y-axis, feet
I_Y	moment of inertia about Y-axis, slugs-feet squared
x_t	tail length (distance from airplane center of gravity to one-third maximum chord point of tail), feet
V_i	correct indicated airspeed $\left\{1703\left[\left(\frac{H-p}{p_o}+1\right)^{0.286}-1\right]^{\frac{1}{2}}\right\}$, miles per hour
H	free-stream total pressure
p	free-stream static pressure
p_o	standard atmospheric pressure at sea level
h_p	pressure altitude, feet
M	free-stream Mach number
V	true airspeed, feet per second
ρ	mass density of air, slugs per cubic foot
q	free-stream dynamic pressure, pounds per square foot
p_u	pressure on upper surface, pounds per square foot
p_l	pressure on lower surface, pounds per square foot
P_R	resultant pressure coefficient $(p_l-p_u)/q$
η_t	tail efficiency factor (q_t/q)
M	pitching moment (stalling moment positive), foot-pounds
M_r	root bending moment (positive when tail tip is deflected upward), foot-pounds
N_t	normal air load on horizontal tail (positive when load is acting upward), pounds

C_m	pitching-moment coefficient $(M/qS_w\bar{c})$
C_{m_t}	tail-moment coefficient due to effective camber $(M_t b_t/q\eta_t S_t^2)$
C_{M_r}	tail root bending-moment coefficient $(M_r/qS_t b_t)$
c_n	section normal-force coefficient
C_{N_t}	tail normal-force coefficient $(N_t/\eta_t q S_t)$
A_Z	the ratio of the net aerodynamic force along the airplane Z-axis (positive when directed upward) to the weight of the airplane
C_L	airplane lift coefficient (WA_Z/qS_w)
α	horizontal surface angle of attack, radians
ϵ	downwash angle, radians
δ_e	elevator angle, radians (unless otherwise noted)
β	sideslip angle (positive when right wing is forward), degrees
θ	angle of pitch, radians
ω_y	pitching velocity $(d\theta/dt)$, radians per second
K	empirical damping factor denoting ratio of damping moment of complete airplane to damping moment of tail alone
F	elevator stick force, pounds
t	time, seconds
τ	aerodynamic time $t/(m/\rho S_w V)$
Δ	this symbol before any quantity other than a subscript denotes the change in value of quantity from time $\tau = 0$
K_1', K_2', K_3'	nondimensional constants occurring in basic differential equation in reference 1
a, b, ν, ν'	functions of the aerodynamic derivatives in the basic differential equations in reference 2

ψ, ψ'	functions of $d\delta_e/dt$ and the aerodynamic derivatives in the basic differential equations in reference 2
$\dot{\alpha}_w$	$d\alpha_w/dt$ or $d\alpha_w/d\tau$
$\dot{\theta}$	$d\theta/dt$ or $d\theta/d\tau$
$\ddot{\alpha}_w$	$d^2\alpha_w/dt^2$ or $d^2\alpha_w/d\tau^2$
$\ddot{\theta}$	$d^2\theta/dt^2$ or $d^2\theta/d\tau^2$

Subscripts

a	airplane
a–t	airplane minus tail
w	wing
t	tail
av	average
exp	experimental
calc	calculated
max	maximum value
bal	for balance
man	in maneuver
$\Delta\delta_e$	due to change in elevator-angle increments at maximum acceleration, such as $\Delta\delta_e = (\Delta\delta_{e_{bal}} - \Delta\delta_{e_{man}})_{\Delta A_{Z_{max}}}$
$\ddot{\theta}$	due to pitching acceleration at $\Delta A_{Z_{max}}$

DESCRIPTION OF AIRPLANE

The test airplane used was a single-engine, pursuit-type, low-wing monoplane with a tractor propeller. Figures 1 and 2 are photographs of the airplane as instrumented for the flight tests; figure 3

is a three-view drawing of the airplane. The pertinent geometric and aerodynamic characteristics of the airplane are given in tables I and II, respectively. The aerodynamic characteristics were obtained from the various sources listed in table II.

INSTRUMENTATION AND PRECISION

A 60-cell pressure recorder was used to measure the resultant pressures over the horizontal tail at the locations given in table III and shown in figure 4. The precision with which the pertinent quantities were believed to be measured in the tests is indicated in the following table:

Item	Estimated accuracy
Normal acceleration	±0.10 g
Elevator angle	±0.50°
Sideslip angle	±1.0°
Airspeed (to 200 mph)	±2½ percent
(above 200 mph)	±1½ percent
Altitude	±300 feet
Tail load (steady, unaccelerated flight)	±50 pounds
(accelerated flight in abrupt maneuvers)	±250 pounds

It should be noted that the estimated precision of the normal acceleration and the tail loads in accelerated flight during abrupt maneuvers is less than that reported in references 5 and 6. This reduction in the estimated accuracy of the measurements results from the fact that in abrupt maneuvers the manometer records were more difficult to correlate at given time instants, and the effect of pitching acceleration on the readings of the accelerometer, displaced slightly aft of the center of gravity, was not accounted for. The pressure-lag characteristics of typical horizontal-tail lines were investigated and it was found that the lag was negligible for the rates of pressure change encountered in this investigation. Other instrumentation of the test airplane and the precision of the

measurements were the same as given in reference 5.

FLIGHT PROGRAM

Six abrupt pull-up push-down maneuvers were made at the flight conditions listed in the following table:

Run	$V_{i_{av}}$	$h_{p_{av}}$	M_{av}	Power	
				Power setting	Estimated[1] brake horsepower
1	358	20250	0.68	Off, propeller in high pitch	−80
2	257	24750	.54	On, full throttle and 3000 rpm	1030
3	376	10150	.59	Off, propeller in high pitch	−130
4	258	9500	.40	Off, propeller in high pitch	−120
5	311	10150	.49	On, 39 in. Hg manifold pressure and 2600 rpm	920
6	313	9850	.49	Off, propeller in high pitch	−120

[1]Estimated from manufacturer's engine power charts.

The maneuver was entered from steady straight flight by pulling abruptly back on the elevator control, holding it fixed until the specified normal acceleration was nearly reached, then pushing the control abruptly forward to pitch the airplane out of the pull-up. It should be noted that the rates of elevator control motion used were the fastest the pilot could apply consistent with the structural limitations of the airplane. At speeds where the limit allowable load factor could be exceeded, the rates of movement and maximum up-elevator deflection were reduced. The measured rates of motion were, in general, slightly less rapid than those indicated in reference 4.

DESCRIPTION OF THE METHODS OF TAIL-LOAD COMPUTATION

In all the methods of computation used it was assumed that:

1. The change in acceleration factor as a result of attitude change is small as compared with that due to a change in angle of attack.

2. The speed is constant during the maneuver.

3. The aerodynamic parameters vary linearly with angle of attack.

4. The effects of structural flexibility may be neglected.

Graphical Method

This method, which is described in detail in reference 1, uses a graphical integration procedure to predict the motions of the airplane following any arbitrary elevator control moment.

The differential equation of motion for a unit elevator deflection can be written as

$$\ddot{\alpha}_w + K_1' \dot{\alpha}_w + K_2' \Delta\alpha_w = K_3' \Delta\delta_e \tag{1}$$

where K_1', K_2', and K_3' are functions of the aerodynamic and geometric characteristics of the airplane. Equation (1) is solved for the unit solutions and the variations of $\Delta\alpha_w$ and $\dot{\alpha}_w$ are determined for the specified elevator motions by employing Duhamel's integral theorem. The increment in effective tail angle of attack at any time during a maneuver, which is related to $\Delta\alpha_w$ and $\dot{\alpha}_w$ by the equation,

$$\Delta\alpha_t = \left\{ \Delta\alpha_w \left[1 - \frac{d\epsilon}{d\alpha_w} - \left(\frac{dC_L}{d\alpha}\right)_a \frac{\rho S_w x_t}{m\sqrt{\eta_t}} \right] - \dot{\alpha}_w \frac{x_t}{V} \left(\frac{d\epsilon}{d\alpha_w} + \frac{1}{\sqrt{\eta_t}} \right) + \frac{d\alpha_t}{d\delta_e} \Delta\delta_e \right\} \tag{2}$$

The tail-load increment is determined from equation (2) by the equation

$$\Delta N_t = \frac{dC_{N_t}}{d\alpha_t} \Delta\alpha_t \, \eta_t \, q \, S_t \tag{3}$$

The load or acceleration factor increment is obtained from the relation

$$\Delta A_Z = \left(\frac{dC_L}{d\alpha}\right)_a \frac{\Delta\alpha_w q}{W/S_w} \tag{4}$$

Tabular Method

This method, a detailed description of which is reported in reference 2, is mathematically similar to that given in reference 1. It is, however, more convenient to use when linear elevator motions are assumed. The general differential equations of motion used in this case, for an elevator deflection proportional to time are

$$\ddot{\alpha}_w - a\dot{\alpha}_w + b\Delta\alpha_w = \psi(t+\nu) \tag{5}$$

$$\ddot{\theta} - a\dot{\theta} + b\theta = \psi'(t+\nu') \tag{6}$$

where a, b, ν, and ν' are functions of simplified aerodynamic derivatives and ψ and ψ' are dependent on the rates of elevator motion and on the derivatives. Equations (5) and (6) are solved for the unit functions of A_Z, α_w, $\dot{\alpha}_w$, $\dot{\theta}$, and $\ddot{\theta}$; and the variations of these quantities are determined for specified or assumed linear elevator motions by a convenient tabular integration procedure. The increment in equivalent tail angle of attack is obtained from the equation,

$$\Delta\alpha_t = \left(1 - \frac{d\epsilon}{d\alpha_w}\right)\Delta\alpha_w + \left(\frac{x_t}{V}\right)\left(\frac{d\epsilon}{d\alpha_w}\right)\dot{\alpha}_w + \frac{x_t}{V\sqrt{\eta_t}}\dot{\theta} + \frac{d\alpha_t}{d\delta_e}\Delta\delta_e \tag{7}$$

It should be noted in the preceding equation that the tail length x_t is considered positive for conventional airplanes, while in the method of reference 1 it is considered negative. The increment in tail load is obtained from equation (7) by the use of equation (3).

The type of linear elevator motion used in the application of this method to compute maximum maneuvering tail loads is shown in figure 5. It is noted that the motions, as specified in reference 2, simulate a pull-up push-down maneuver. The rates of motion, as indicated in the figure, were based for the most part on the data of reference 2 and reference 4. In contrast with the computations using the graphical method where the elevator motion used was identical to that measured in flight, the maximum up-elevator angle was adjusted so that the maximum experimental value of ΔA_Z was just reached in the design maneuver. The comparisons here then are based upon common or identical values of $\Delta A_{Z_{max}}$. Motions with both a 0.2-second and 0.4-second elevator reversal were included because, upon occasion, the designer may be undecided as to the exact rate of reversal to use. This being the case, and since the reversal rate is probably

the most important variable in establishing the linear motions, it was believed to be of interest to know quantitatively the effect of a change in the reversal rate on the calculated results.

Abbreviated Methods

In one of these methods the tabular integration method is used to establish the elevator-angle increment $\Delta\delta_{e_{man}}$ corresponding to the maximum value of ΔA_Z in the maneuver for a 0.2-second reversal of the elevator. The elevator-angle increment for balance at $\Delta A_{Z_{max}}$ is determined from the equation

$$\Delta\delta_{e_{bal}} = \frac{\Delta C_L \Delta A_{Z_{max}} \left(\frac{dC_m}{dC_L}\right)_a}{(dC_m/d\delta_e)_a} \tag{8}$$

Assuming that the maximum maneuvering tail-load increment occurs at $\Delta A_{Z_{max}}$, the load increment is computed from the equation

$$\Delta N_{t_{man}} = \Delta N_{t_{bal}} + \frac{dC_{N_t}}{d\delta_e} (\Delta\delta_{e_{man}} - \Delta\delta_{e_{bal}})_{\Delta A_{Z_{max}}} q\eta_t S_t \tag{9}$$

where $\Delta N_{t_{bal}}$ is computed by the use of the equation given in reference 5 for ΔC_L corresponding to $\Delta A_{Z_{max}}$ in the maneuver.

A second abbreviated procedure was used in which the value of angular pitching acceleration is determined at $\Delta A_{Z_{max}}$ by establishing the elevator motion with a 0.2-second elevator reversal, as for the previous method for the desired maximum acceleration factor increment, and by computing the pitching accelerations associated with this elevator motion. The maximum maneuvering tail-load increment is again assumed to occur at $\Delta A_{Z_{max}}$ so that

$$\Delta N_{t_{man}} = \Delta N_{t_{bal}} + \frac{I_Y \ddot{\theta}}{x_t} \tag{10}$$

where $\Delta N_{t_{bal}}$ is determined as before from the equation given in reference 5.

RESULTS

Experimental Data

The experimental results including time histories of basic flight variables, total tail-load and root bending-moment increments, acceleration-factor and elevator-angle increments, and the load distributions are presented in figures 6 to 9. Most of the data shown in figures 6(a) to 6(f) are used subsequently to compute the tail-load increment variations following specified elevator motions.

In figures 7(a) to 7(f) the experimental tail-load and root bending-moment increments are shown for the several runs. These increments were determined by subtracting from the measured loads and bending moments at any instant the balancing loads and moments at time $\tau = 0$. (See fig. 6.) The measured elevator-angle and acceleration-factor increments (figs. 8(a) to 8(f)) were determined in a similar manner. The experimental resultant pressure distributions are shown in figures 9(a) to 9(f)). For purposes of comparison with computed results these distributions correspond to the time in each run when the calculated load increments based on the experimental elevator motions are a maximum. In this way differences in elevator angles which would distort the comparisons of the load distributions were avoided.

Computed Data

From the basic flight data presented in figure 6 and from the aerodynamic and geometric characteristics of the test airplane, the calculated variations of tail-load and root bending-moment increments (fig. 7) were determined. The root bending-moment increments were determined by multiplying one-half the computed tail-load increments by the calculated distance to the center of pressure which was assumed at the centroid of area of one side of the tail. The computed or assumed variations of elevator-angle and acceleration-factor increment are shown in figure 8. The computed tail-load distributions shown in figure 9 were determined by the methods of references 7 and 8.

A summary of the experimental and the computed results is presented in tables IV and V.

In the computations, Mach number effects on most of the aerodynamic parameters were not included, since the load calculations for the one test airplane of reference 3 which attained a Mach number of 0.61 showed no appreciable compressibility effects on the computed load increments. In the present investigation only run 1 was made at a higher Mach number ($M = 0.68$).

DISCUSSION

As previously pointed out, the measured and computed results are compared either upon the basis of identical elevator motions or approximately the same values of maximum normal acceleration. In the former case, the purpose of the comparison is to provide a check on the validity of the methods currently available for predicting maximum maneuvering tail loads from known or prescribed elevator motions. In the latter, the reason for the comparison is to determine the extent to which tail loads computed by use of estimated linear elevator motions or abbreviated methods, agree with tail loads measured in abrupt pull-up push-down maneuvers as made by a pilot in flight.

Comparisons Made to Check Validity of Rigorous Methods of Computation

In general, as seen in figure 7 and table IV(A), the results of comparisons made on the basis of identical elevator motions show that relatively good agreement is obtained between the maximum measured and computed tail-load increments. The comparisons also show, however, that where the basic assumption of the methods of computation are violated, agreement between computed and measured values may not be good. For example, in run 2, where the lift coefficient reached a value of nearly 1.2 at a Mach number of 0.54 the lack of close agreement is attributed to the fact that the airplane was stalled at this moderate Mach number; consequently, the basic assumption that the aerodynamic parameters varied linearly with angle of attack was not valid for this run. For the same reason lack of agreement might be expected in run 4 in which a lift coefficient of 1.4 was reached at a Mach number of about 0.41. In run 5, however, in which a lift coefficient of about 1.2 was reached at a lower Mach number than that reached in run 2, namely 0.49, the agreement between computed and measured values was good. The results presented in table IV(A) show that the maximum computed up-load increments deviate from the experimental results an average of 11.4 percent for five of the six runs investigated. (Run 2 was not included in the average deviation because of the stalled condition.)

The agreement shown in figure 8 between the maximum experimental and the maximum computed wing-load or acceleration-factor increments is not as satisfactory as was the case for the tail-load increments. It is believed that part of the discrepancy can be attributed to possible errors in certain aerodynamic parameters used in the calculation, in particular the airplane lift-curve slope. This possibility is indicated by the fact that, while a value of $(dC_L/d\alpha)_a$ of 4.12

was used in the computations for the present investigation, unpublished data (which were not available at the time most of the computations for this report were made) from the Ames 16-foot high-speed wind tunnel indicated a value of 4.80 at a Mach number of 0.40. Calculations showed that while this difference in $(dC_L/d\alpha)_a$ had little effect on the tail-load increments, it had an appreciable effect on the values of the computed acceleration-factor increments. The use of the Ames 16-foot wind-tunnel value of $(dC_L/d\alpha)_a$ would have reduced the average discrepancy between computed and actual values of ΔAz_{max} from about 20 to about 15 percent. It is important to note that, while the change in $(dC_L/d\alpha)_a$ did not affect the tail-load increments appreciably, it would have a large effect in cases where the elevator motions are varied to produce specified values of ΔAz_{max}. This distinction is illustrated further in a later section of this report.

These results are in general agreement with those presented in reference 3 which showed, in a majority of the comparisons, that the maximum computed wing- and tail-load increments for several airplanes agreed quite well with the measured values. Where poor agreement was obtained, the trouble was traced either to poor quantitative knowledge of the value of certain aerodynamic parameters or to violations of the assumptions upon which the methods of computation are based.

It appears, then, that methods currently available for predicting maximum maneuvering tail loads from prescribed elevator motions are valid and can be used with assurance, provided the aerodynamic parameters are accurately known. It should be recognized that these methods would not be valid for predicting tail loads in maneuvers where the basic assumptions common to these methods were not applicable.

Comparisons Made to Check Validity of Using Estimated Linear Elevator Motions

This type of comparison is made to permit an over-all appreciation of the accuracy with which maneuvering tail loads may be expected to be computed for given values of load factor. Comparisons are made between loads measured and those computed in pull-up push-down maneuvers in which the elevator motions are assumed to be linear (method of reference 2).

As is shown in table IV(A), where comparisons are made on the basis of the same values of ΔAz_{max}, the maximum tail-load increments computed using estimated linear elevator motions with 0.2-second and 0.4-second reversal deviate from the experimental results an average of 41.3 and 21.4 percent, respectively.

It appears that the use of estimated linear elevator motions consistent with the experimental values of ΔAz_{max}, instead of the actual motions produced increases in the average deviations of 29.9 and 10.0 percent, respectively, for the assumed elevator motions with 0.2-second and 0.4-second reversals. Analysis indicates, however, that most of the increased deviations are traceable to possible errors in some of the aerodynamic parameters.

Since, for design purposes, the fastest possible rate of reversal would generally be used for predicting maximum maneuvering tail loads, subsequent discussion will be confined to analysis of the results computed using the linear elevator motions with a 0.2-second reversal. (As was previously noted, the linear motion with 0.4-second reversal, was included to show the effect of a change in the reversal rate on the computed results.)

To illustrate the effects of inconsistencies or errors in the aerodynamic parameters consider, for example, the effect of a possible error in $(dC_L/d\alpha)_a$ discussed initially in the previous section, where comparisons were based on identical elevator motions. It can be shown that for a constant value of ΔAz_{max}, an increase in $(dC_L/d\alpha)_a$ from 4.12 to 4.80 (as indicated by Ames 16-foot wind-tunnel tests) would reduce the average deviation of the computed tail loads from the measured results from 41.3 to 23.3 percent. This was based on computations which were repeated for one run using a value of 4.80 for the airplane lift-curve slope. It can be further shown that a small additional error was introduced into the tail-load computations because the values of $(dC_m/d\alpha)_{a-t}$ and $(dC_m/d\alpha)_a$ obtained from two equally valid sources were not determined with sufficient accuracy to permit a perfect check of one value with the other. Results of a large number of studies presented in reference 2 show that, depending on whether ΔAz_{max} or the elevator motion is held constant, the maximum maneuvering tail load will increase either about 2 or 5 percent, respectively, for a 2-percent (the degree of inconsistency in $(dC_m/d\alpha)_a$ obtained from the two sources) movement aft of the airplane center of gravity. Thus, it can be shown that the use of a consistent value of $(dC_m/d\alpha)_a$ in the present case would further reduce the difference between the average computed load deviations using the measured and the estimated linear elevator motions. If the value given in reference 5 is assumed correct, the average deviation of the computed results (using linear elevator motions) from the measured load increments would be reduced from 23.3 to 21.3 percent. Assuming that the value of $(dC_m/d\alpha)_a$ given in reference 9 is correct, the average deviation from the experimental load increments of the values computed using the experimental elevator motions would be increased from 11.4 to 16.4 percent. From the foregoing, it appears that the difference between the average computed load deviations using the estimated linear and the measured

elevator motions can be reduced from 29.9 to either 9.9 or 6.9 percent by accounting for possible errors or inconsistencies in the values of $(dC_L/d\alpha)_a$ and $(dC_m/d\alpha)_a$.

Analysis of the present results indicates, then, that the estimated linear elevator motions with a 0.2-second reversal are practically as satisfactory as the actual elevator motions for computing maximum maneuvering tail loads in abrupt pull-up push-down maneuvers.

Comparisons Made to Check Validity of Abbreviated Methods of Prediction

Comparison is made in table V(A) between the maximum experimental tail-load increments and the maximum values computed by the two abbreviated methods previously described. Although not as rigorous as the more complete graphical and tabular methods, they gave results which are considered fairly satisfactory. Average deviations between the measured values and those computed using $\Delta N_{t_{bal}} + N_{t_{\Delta\delta_e}}$ and $\Delta N_{t_{bal}} + N_{t_{\ddot{\theta}}}$ were 14.3 and 22.4 percent, respectively.

It should be noted that the computations could be further shortened by estimation of the maneuvering elevator angle at $\Delta A_{Z_{max}}$ and and the pitching acceleration at $\Delta A_{Z_{max}}$. As a first approximation, $\Delta\delta_{e_{man}}$ at $\Delta A_{Z_{max}}$ was assumed one-half the elevator-angle increment required for balance. For the test airplane, this resulted in computed tail loads which predicted the actual within an average of 13 percent for the six runs. For the special case where the center of gravity is located at the position for neutral stick-fixed stability, the aforementioned method would be invalidated, since $\Delta\delta_{e_{bal}}$ would be zero and the maneuvering load so computed would be equal to the balancing load. Similarly, an assumption of a common pitching acceleration at $\Delta A_{Z_{max}}$ of 4 radians per second squared for the six runs resulted in an average deviation of the computed from the measured load increments of about 20 percent. Caution should be exercised in generalizing these results, however, since possible errors in the aerodynamic parameters used (as indicated by previous discussion) would change the average deviations significantly. These changes would be of the order of about -5 percent to 20 percent for the extreme cases.

Although these results cannot be conclusively considered representative (since they were obtained on only one airplane) they may indicate the accuracy to be expected of the methods if they are used to compute design maneuver loads for any airplane of the same general configuration as that of the test airplane. The results

obtained on the test airplane are considered sufficiently accurate for preliminary design estimates.

Effects of Speed on Load Comparisons

A comparison between the computed and the experimental limit maneuvering and balancing tail loads is included as figure 10 for a range of indicated airspeed to show where maximum maneuvering loads may be encountered, and to indicate the relative magnitude of the balancing and maneuvering loads as measured and as computed. It should be noted that the computed maneuvering loads were obtained using values of 4.12 and −0.124 for the airplane lift-curve and moment-curve slopes, respectively. It was indicated previously that better agreement with the measured results would have been obtained if a good quantitative knowledge was had of these two pertinent aerodynamic parameters. The balancing loads for the limit load factor of 7.33 and for zero load factor were obtained from the data of reference 5. The computed and experimental maneuvering tail-load variations for the load factor of 7.33 were obtained by fairing through the individual load increments reduced to a common $\Delta A_{Z_{max}}$ of 7.33 and adding to the resulting curves the corresponding balancing loads at $A_Z = 0$. The individual data points are included to show the relative amount of scatter, which is considerable in the case of the measured loads and the loads computed using the measured elevator motions. This scatter results, of course, from variations in the severity of the experimental elevator motions used. In accord with the data of reference 2, the maneuvering loads computed by the several methods decrease from the neighborhood of the upper left-hand corner of the V-g diagram from about 15 to 25 percent over the airspeed range covered. The measured loads increase up to about 300 miles per hour, then fall off quite rapidly at higher speeds.

Comparisons Between Measured and Computed Root Bending-Moment Increments

A comparison between the maximum experimental and the maximum calculated tail bending-moment increments based on the measured and the computed elevator motions is made in table IV(B). It is shown that if the experimental elevator functions are known, the average deviation of the computed bending-moment increments from the measured results if 7.1 percent compared to 11.4 percent for tail loads. The maximum bending-moment increments, based on the linear elevator motions with reversal occurring in 0.2 second and 0.4 second adjusted to give values of ΔA_Z identical with those measured, deviate an average of 28.3 and 14.2 percent, respectively, from the experimental values; whereas the corresponding tail-load deviations were 41.3 and 21.4 percent.

The maximum root bending-moment increments calculated by the use of the two shortened procedures are compared with the experimental results in table V(B). The bending-moment increments based on the computed elevator-angle change at ΔAz_{max} deviate an average of 9.3 percent from the measured values, while those based on the calculated value of pitching acceleration at ΔAz_{max} are in error an average of 13.2 percent.

It will be noted from the above comparisons that the computed bending-moment increments are generally less conservative than the computed load increments. This results from the fact that the computed lateral distance to the center of pressure is inboard of the measured values. Figure 11 presents the experimental and calculated distances to the center of pressure as a function of tail normal-force coefficient C_{N_t}. As previously noted, the computed value was assumed to be located at the centroid of area of one side of the tail. It should be noted from figure 11 that the experimental value appears to move slightly inboard with an increase in C_{N_t}. Furthermore, the computed distance to the center of pressure is inboard of the measured values an average of about 10 percent.

Evaluation of Methods for Predicting Load Distributions

The previous sections of this report have dealt with the evaluation of several methods for computing the maximum horizontal-tail loads and root bending-moment increments in abrupt maneuvers. Having ascertained the accuracy with which the over-all loads and bending moments were determined, it seems desirable to determine how closely the calculated load distributions compare with the experimental distributions. This was done by distributing the maximum computed over-all loads based on the experimental elevator motions over the tail span by assuming unit span loads proportional to the tail chord. The methods of references 7 and 8 were used to distribute the unit span loads over the tail chord, and the resulting distributions were compared with the experimental results at the same time. This was done so that the elevator angles would be the same for the computed and measured distributions.

The comparisons shown in figure 9 indicate, in general, fairly good agreement at the midspan stations. At the spanwise stations adjacent to the fuselage and tip, however, the computed chordwise load distributions generally show higher peaks near the stabilizer leading edge for the former, and lower peak loads for the latter stations, as compared with the experimental results. One possible reason for this is the effect of the fuselage in causing a reduction of load at the inboard tail stations. For a given load, the resulting outward shift of the center of pressure would cause some of the discrepancies between the calculated and experimental distributions. The agreement shown between the computed and measured span loading

curves is considered fairly good, although it is evident that the computed total loads for run 2 and run 4 are considerably higher than the actual values. Better agreement was not obtained because present design practice incorrectly assumes that the unit span loads are proportional to the tail chord.

CONCLUSIONS

Comparisons have been made between the horizontal-tail loading obtained in six pull-up push-down maneuvers in flight on a representative pursuit-type airplane and the computed tail loading based on several rational procedures. On the basis of these comparisons it was concluded that for airplanes of the same general configuration as the test airplane:

1. Methods currently available for predicting maximum maneuvering tail loads from prescribed elevator motions are valid and can be used with assurance, provided the aerodynamic parameters are accurately known.

2. Computations of tail load based on linear elevator motion in a pull-up push-down maneuver with a 0.2-second elevator reversal may be expected to give very nearly the same values of maneuvering tail load as those that would be measured in actual pull-up push-down maneuvers at identical values of $\Delta A_{Z_{max}}$, provided aerodynamic parameters used in the computations are accurate.

3. The maximum tail-load increments computed by the use of the two abbreviated methods will be in fairly good agreement with actual values and would, in general, be sufficiently accurate for preliminary design studies.

4. For a given maximum maneuvering tail load, the maximum computed root bending moment will be approximately 10 percent less than the value that would be obtained in flight, as the computed distance to the center of pressure would be about 10 percent inboard of the actual value.

5. The computed chordwise and spanwise tail-load distributions will be in fairly good agreement with actual values, provided the computed values of over-all loads are in close agreement with actual values. Better agreement would be expected if, in distributing the load along the span, the effects of the fuselage were considered in addition to the variation of tail chord.

Ames Aeronautical Laboratory,
National Advisory Committee for Aeronautics,
Moffett Field, Calif.

REFERENCES

1. Pearson, Henry A.: Derivation of Charts for Determining the Horizontal Tail Load Variation with any Elevator Motion. NACA ARR, Jan. 1943.

2. Kelley, Joseph, Jr., and Missal, John W.: Maneuvering Horizontal Tail Loads. Army Air Forces Technical Rep. No. 5185, January 25, 1945. (Now available from Department of Commerce as PB No. 49611.)

3. Matheny, Cloyce E.: Comparison Between Calculated and Measured Loads on Wing and Horizontal Tail in Pull-Up Maneuvers. NACA ARR No. L5H11, 1945.

4. Beeler, De E.: Maximum Rates of Control Motion Obtained From Ground Tests. NACA RB No. L4E31, 1944.

5. Sadoff, Melvin, Turner, William N., and Clousing, Lawrence A.: Measurements of the Pressure Distribution on the Horizontal-Tail Surface of a Typical Propeller-Driven Pursuit Airplane in Flight. I – Effects of Compressibility in Steady Straight and Accelerated Flight. NACA TN No. 1144, 1947.

6. Sadoff, Melvin and Clousing, Lawrence A.: Measurements of the Pressure Distribution on the Horizontal Tail Surface of a Typical Propeller-Driven Pursuit Airplane in Flight. II – The Effect of Angle of Sideslip and Propeller Operation. NACA TN No. 1202, 1947.

7. Allen, H. Julian: Calculation of the Chordwise Load Distribution Over Airfoil Sections with Plain, Split, or Serially Hinged Trailing-Edge Flaps. NACA Rep. No. 634, 1938.

8. Abbot, Ira H., von Doenhoff, Albert E., and Stivers, Louis S. Jr.: Summary of Airfoil Data. NACA ACR No. L5C05, 1945.

9. Turner, William N., Steffen, Paul J., and Clousing, Lawrence A.: Compressibility Effects on the Longitudinal Stability and Control of a Pursuit-Type Airplane as Measured in Flight. NACA ACR No. 5I13, 1945.

10. Silverstein, Abe, and Katzoff, S.: Aerodynamic Characteristics of Horizontal Tail Surfaces. NACA Rep. No. 688, 1940.

11. Gilruth, R. R., and White, M. D.: Analysis and Prediction of Longitudinal Stability of Airplanes. NACA Rep. No. 711, 1941.

12. White, Maurice D.: Estimation of Stick-Fixed Neutral Points of Airplanes. NACA CB No. L5C01, 1945.

13. Ames, Milton B., Jr., and Sears, Richard I.: Determination of Control-Surface Characteristics from NACA Plain-Flap and Tab Data. NACA Rep. No. 721, 1941.

TABLE I.- GEOMETRIC CHARACTERISTICS OF TEST AIRPLANE

Item	Value
Gross wing area (S_w), sq ft	213.22
Gross horizontal-tail area (S_t), sq ft	40.99
Tail incidence, with reference to thrust axis, deg	2.25
Average airplane weight during test run (W), lb	7600
Design gross weight	7406
Wing span (b_w), ft	34.0
Horizontal-tail span (b_t), ft	13.0
Moment of inertia of airplane (I_Y), slug-ft^2	6380
Mass of airplane (m), slugs	236
Radius of gyration of airplane (K_Y), ft	5.2
Tail length (x_t), ft	±15.0
Mean aerodynamic chord ($\bar{c}$), ft	6.72
Center-of-gravity location, percent $\bar{c}$	30.3

NATIONAL ADVISORY
COMMITTEE FOR AERONAUTICS

TABLE II.- AERODYNAMIC CHARACTERISTICS OF TEST AIRPLANE

Item	Value	Source
Slope of airplane lift curve $(dC_L/d\alpha)_a$, radian	4.12	Langley full-scale tunnel tests
Slope of tail-plane lift curve $(dC_{N_t}/d\alpha_t)$, radian	3.38	Reference 10
Downwash factor $(d\epsilon/d\alpha_w)$	0.49	References 11 and 12
Tail efficiency factor (η_t)	1.00	Assumed
Empirical damping factor (K)	1.10	Reference 1
Empirical damping factor (K)	1.25	Reference 2
Elevator effectiveness $(dC_{N_t}/d\delta_e)$, radian	1.89	Reference 10
Tail moment change with elevator angle $(dC_{m_t}/d\delta_e)$, radian	0.532	Reference 13
Slope of airplane moment curve minus tail $\left[(dC_m/d\alpha)_{a-t}\right]$, radian	0.531	Reference 5
Slope of airplane moment curve $\left[(dC_m/d\alpha)_a\right]$, radian	-0.124	Reference 9
Airplane moment change with elevator angle $(dC_m/d\delta_e)$, radian	-0.830	Unpublished data on file at laboratory
Change of tail angle of attack with elevator angle $(d\alpha_t/d\delta_e)$	0.56	Reference 10

NATIONAL ADVISORY COMMITTEE FOR AERONAUTICS

TABLE III.- ORDINATES AT PRESSURE ORIFICES ON HORIZONTAL TAIL OF TEST AIRPLANE

[All values are in percent of chord]

Orifice	Row A				Row B				Row C				Row D			
	Upper surface		Lower surface		Upper surface		Lower surface		Upper surface		Lower surface		Upper surface		Lower surface	
	Station	Ordinate	Station	Ordinate	Station	Ordinate	Station	Ordinate	Station	Ordinate	Station	Ordinate	Station	Ordinate	Station	Ordinate
Left side																
1	1.44	1.55	1.55	1.55	2.57	1.70	2.84	1.70	1.61	1.24	1.24	1.14	2.08	1.40	2.21	1.43
2	10.15	3.51	9.37	3.51	10.43	3.23	9.88	3.27	7.30	2.43	7.08	2.48	25.04	3.15	24.98	3.09
3	30.96	4.48	30.96	4.64	31.89	4.11	31.95	4.21	20.35	3.28	20.25	3.38	46.14	2.93	46.34	2.93
4	47.10	4.13	46.44	4.23	42.61	2.95	42.66	3.91	31.06	3.35	33.79	3.45	57.56	2.11	57.72	2.11
5	57.48	3.80	57.28	3.72	54.55	3.55	54.65	3.52	46.91	3.03	46.71	3.01	70.60	1.95	70.99	1.95
6	62.54	1.80	62.54	1.86	59.77	1.52	59.88	1.86	57.29	2.19	57.44	2.36	79.80	1.40	80.00	1.37
7	68.98	2.79	69.04	2.89	68.93	2.61	68.98	2.84	67.58	2.09	68.05	1.99	- - -	- -	- - -	- -
8	82.64	1.65	82.68	1.75	80.68	1.66	80.84	1.73	83.73	1.17	83.73	.99	- - -	- -	- - -	- -
Right side																
1	1.34	1.45	1.51	1.45	2.02	1.59	2.40	1.70	1.96	1.49	2.43	1.49	1.98	1.50	2.02	1.24
2	10.10	3.57	10.03	3.45	10.06	3.27	10.43	3.29	9.80	3.00	10.12	2.75	25.24	3.24	26.18	3.09
3	30.90	4.55	30.86	4.47	31.75	4.20	31.86	4.08	35.56	3.66	36.08	3.29	45.37	2.93	45.85	3.06
4	47.70	4.10	47.22	4.16	43.08	3.92	43.08	3.83	49.02	3.29	49.28	3.14	58.86	2.44	58.37	1.95
5	57.70	3.70	57.54	3.74	54.33	3.63	54.42	3.51	60.13	2.75	60.42	2.14	71.54	2.11	70.93	1.95
6	63.33	2.17	62.40	1.86	59.36	1.95	59.52	1.59	71.11	2.17	71.24	1.91	80.16	1.63	80.03	1.37
7	68.67	2.77	68.60	2.92	68.89	2.74	69.14	2.72	84.97	1.20	84.97	1.18	- - -	- -	- - -	- -
8	82.25	1.80	82.11	2.05	78.23	2.02	78.28	1.97	- - -	- -	- - -	- -	- - -	- -	- - -	- -
9	- - -	- -	- - -	- -	86.96	1.36	86.73	1.36	- - -	- -	- - -	- -	- - -	- -	- - -	- -

NATIONAL ADVISORY
COMMITTEE FOR AERONAUTICS

TABLE IV.- COMPARISON BETWEEN THE MAXIMUM POSITIVE EXPERIMENTAL TAIL-LOAD AND ROOT BENDING-MOMENT INCREMENTS AND THE CALCULATED VALUES BASED ON THE EXPERIMENTAL ELEVATOR MOTIONS AND THE COMPUTED ELEVATOR MOTIONS WITH 0.2-SECOND AND 0.4-SECOND REVERSALS OF THE ELEVATOR

(A) LOADS

Run	Measured			Calculated (using measured elevator motions)		Calculated (using estimated linear elevator motions)			
	Left	Right	Total	Total	Deviation (percent)	Total for δ_e motion with 0.2-second reversal	Deviation (percent)	Total for δ_e motion with 0.4-second reversal	Deviation (percent)
1	1684	1793	3477	3960	13.9	4309	23.9	3648	4.9
2	1232	1215	2447	3490	42.6[1]	3545	44.7	3183	30.0
3	1173	1269	2442	2585	5.9	3932	61.5	3313	35.9
4	1569	1735	3304	4250	28.6	5112	54.7	4346	31.6
5	2003	1928	3931	4210	7.1	5741	46.1	4761	21.1
6	2542	2514	5056	5130	1.5	5913	16.9	4812	-4.8
Average deviation	——	——	——	——	11.4	——	41.3	——	21.4

(B) BENDING MOMENTS

Run	Measured		Calculated (using measured elevator motions)		Calculated (using estimated linear elevator motions)			
	Left	Right	Left or right	Deviation (percent)	Left or right for δ_e motion with 0.2-second reversal	Deviation (percent)	Left or right for δ_e motion with 0.4-second reversal	Deviation (percent)
1	5512	5622	5750	2.3	6250	11.2	5295	-5.8
2	3918	3902	5060	29.2[1]	5145	31.4	4625	18.0
3	3760	3952	3755	-5.0	5705	44.3	4805	21.6
4	5118	5172	6165	19.2	7415	43.3	6305	21.9
5	6412	6390	6110	-4.7	8330	29.9	6905	7.7
6	7796	7790	7445	-4.5	8575	10.0	6985	-10.4
Average deviation	——	——	——	7.1	——	28.3	——	14.2

[1]Not included in average deviation because airplane was definitely stalled during this run.

TABLE V.– COMPARISON AT THE SAME VALUES OF ΔZ_{max} OF THE MAXIMUM POSITIVE EXPERIMENTAL TAIL-LOAD AND ROOT BENDING-MOMENT INCREMENTS WITH THOSE COMPUTED BY THE USE OF TWO ABBREVIATED METHODS.

(A) LOADS

Run	Experimental			Calculated			
	Left	Right	Total	Total for $\Delta N_{t_{bal}} + N_{t_{\Delta\delta_e}}$	Deviation (percent)	Total for $\Delta N_{t_{bal}} + N_{t_{\ddot{\theta}}}$	Deviation (percent)
1	1684	1793	3477	3480	0	3780	8.7
2	1232	1215	2447	2800	14.4	2880	17.7
3	1173	1269	2442	3210	31.6	3420	40.3
4	1569	1735	3304	3860	16.8	4530	37.1
5	2003	1928	3931	4490	14.2	5030	28.0
6	2542	2514	5056	4630	-8.4	5190	2.6
Average deviation	——	——	——	——	14.3	——	22.4

(B) BENDING MOMENTS

Run	Experimental		Calculated			
	Left	Right	Left or right for $\Delta M_{r_{bal}} + M_{r_{\Delta\delta_e}}$	Deviation (percent)	Left or right for $\Delta M_{r_{bal}} + M_{r_{\ddot{\theta}}}$	Deviation (percent)
1	5512	5622	5050	-10.2	5480	-2.5
2	3918	3902	4070	3.9	4180	6.7
3	3760	3952	4660	17.9	4960	25.5
4	5118	5172	5600	8.3	6570	27.0
5	6412	6390	6510	1.5	7300	13.8
6	7796	7790	6720	-13.8	7530	-3.4
Average deviation	——	——	——	9.3	——	13.2

NATIONAL ADVISORY COMMITTEE FOR AERONAUTICS

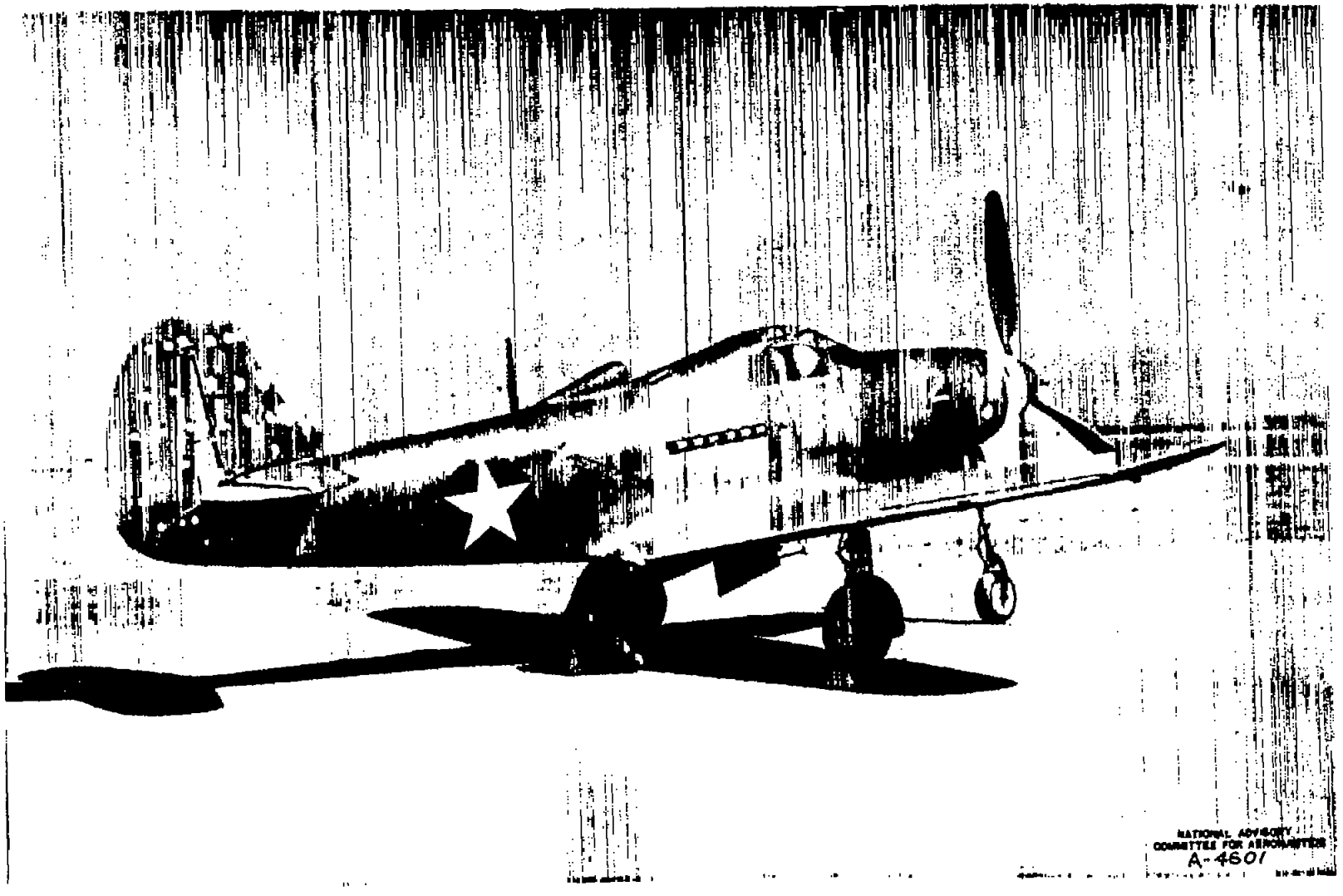

Figure 1.- Three-quarter rear view of test airplane as instrumented for tail-load flight tests.

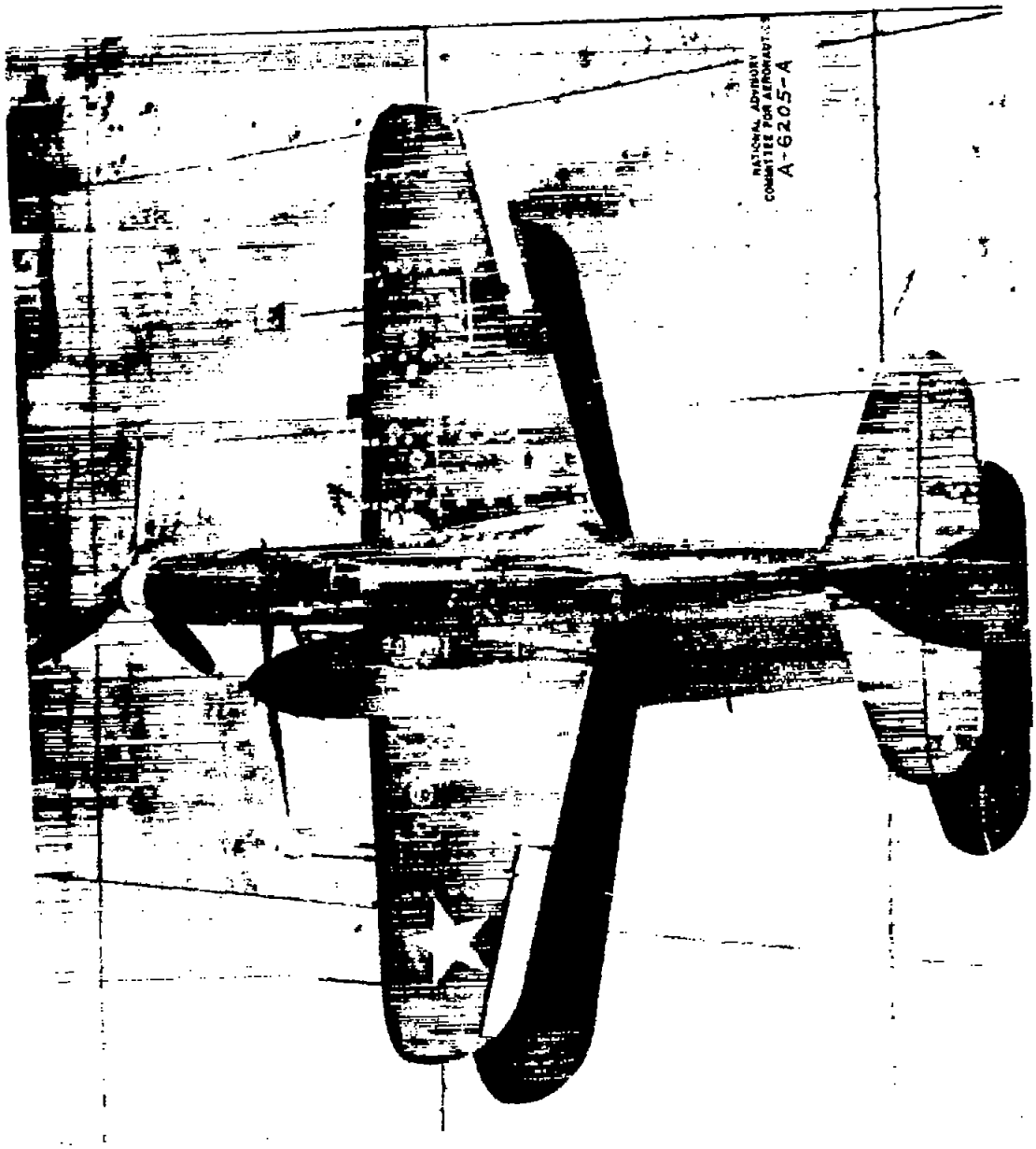

Figure 2.- Top view of test airplane as instrumented for flight tests.

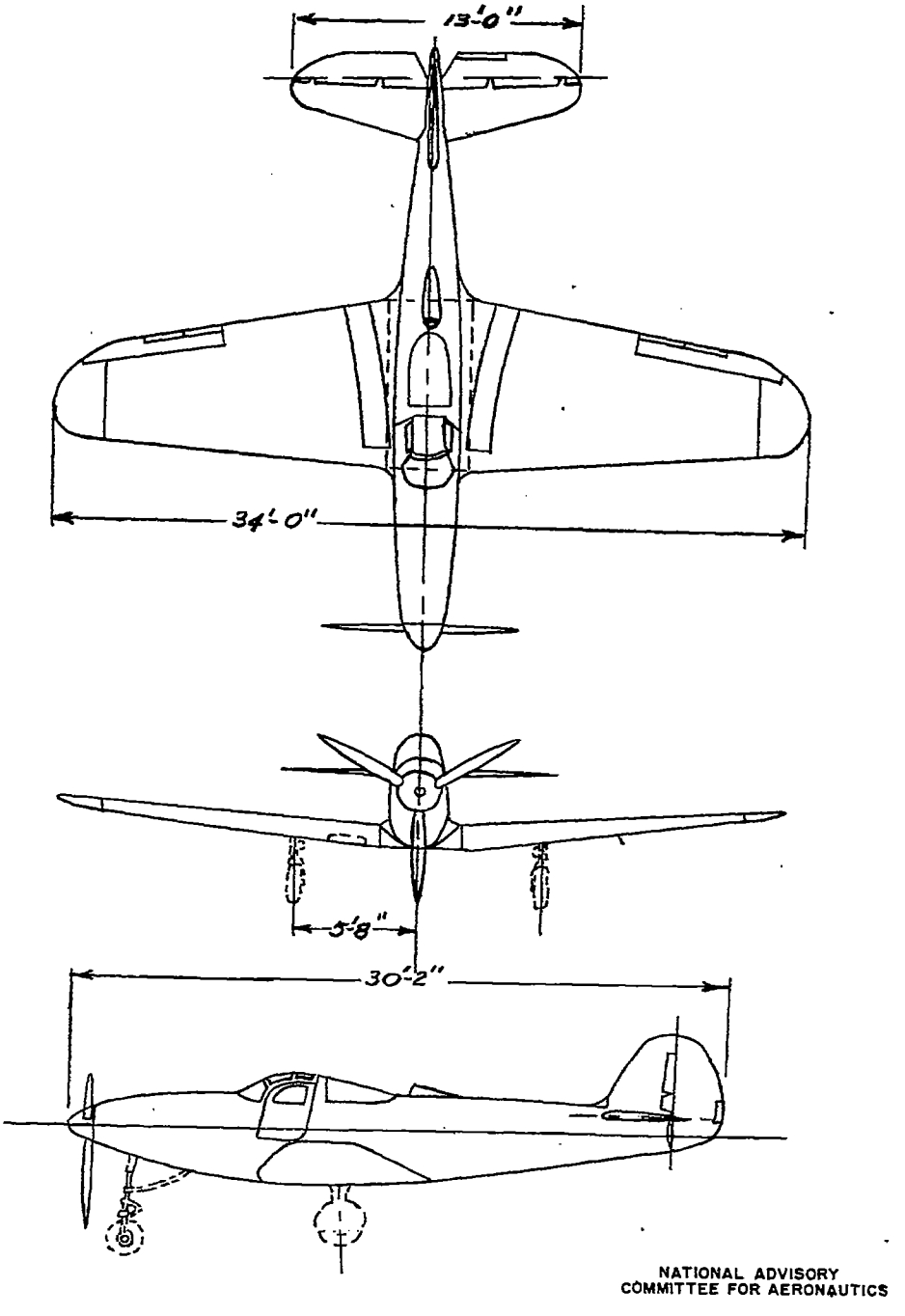

Figure 3. — Three-view drawing of the test airplane.

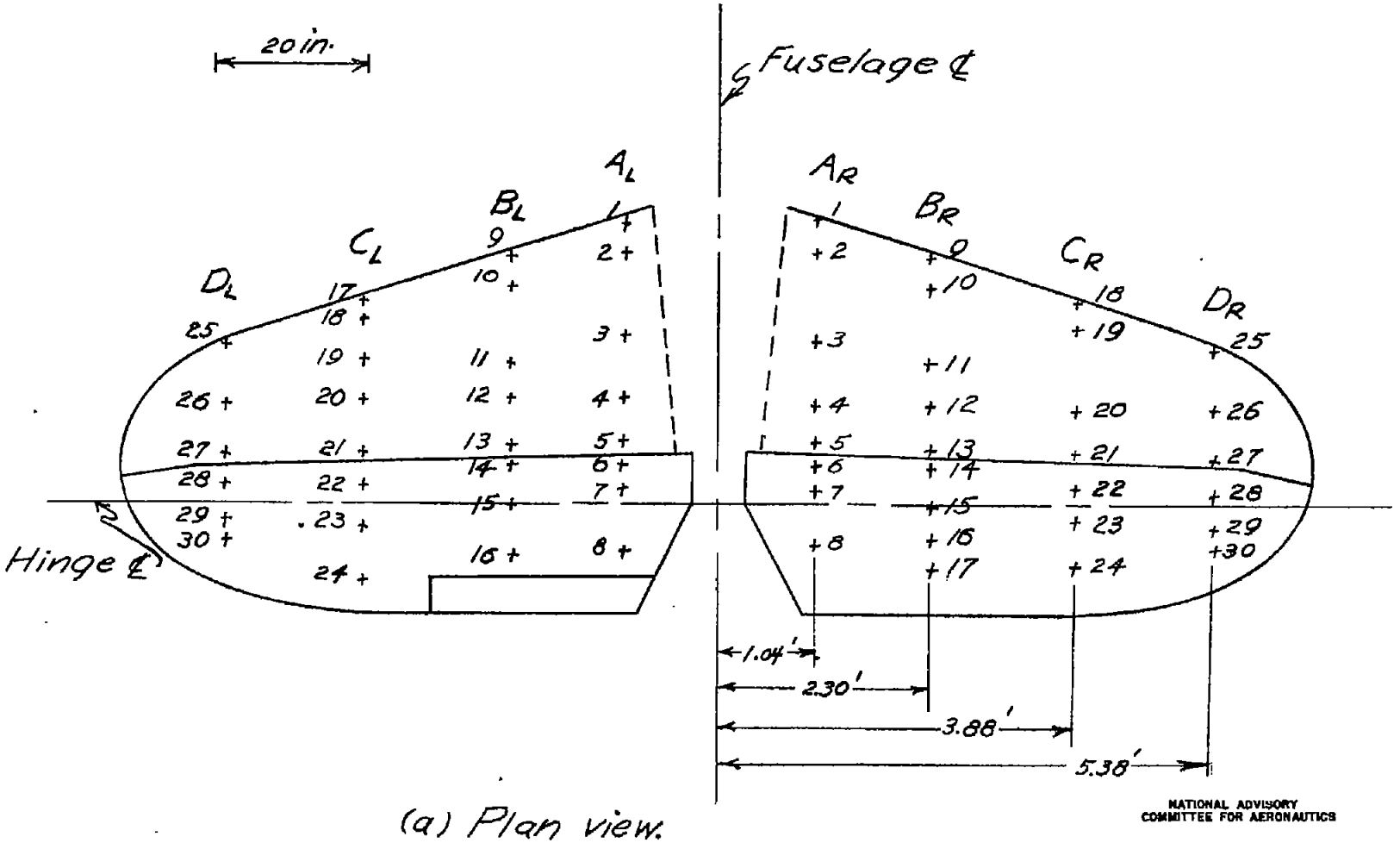

(a) Plan view.

Figure 4. - Orifice locations on horizontal tail. Test airplane.

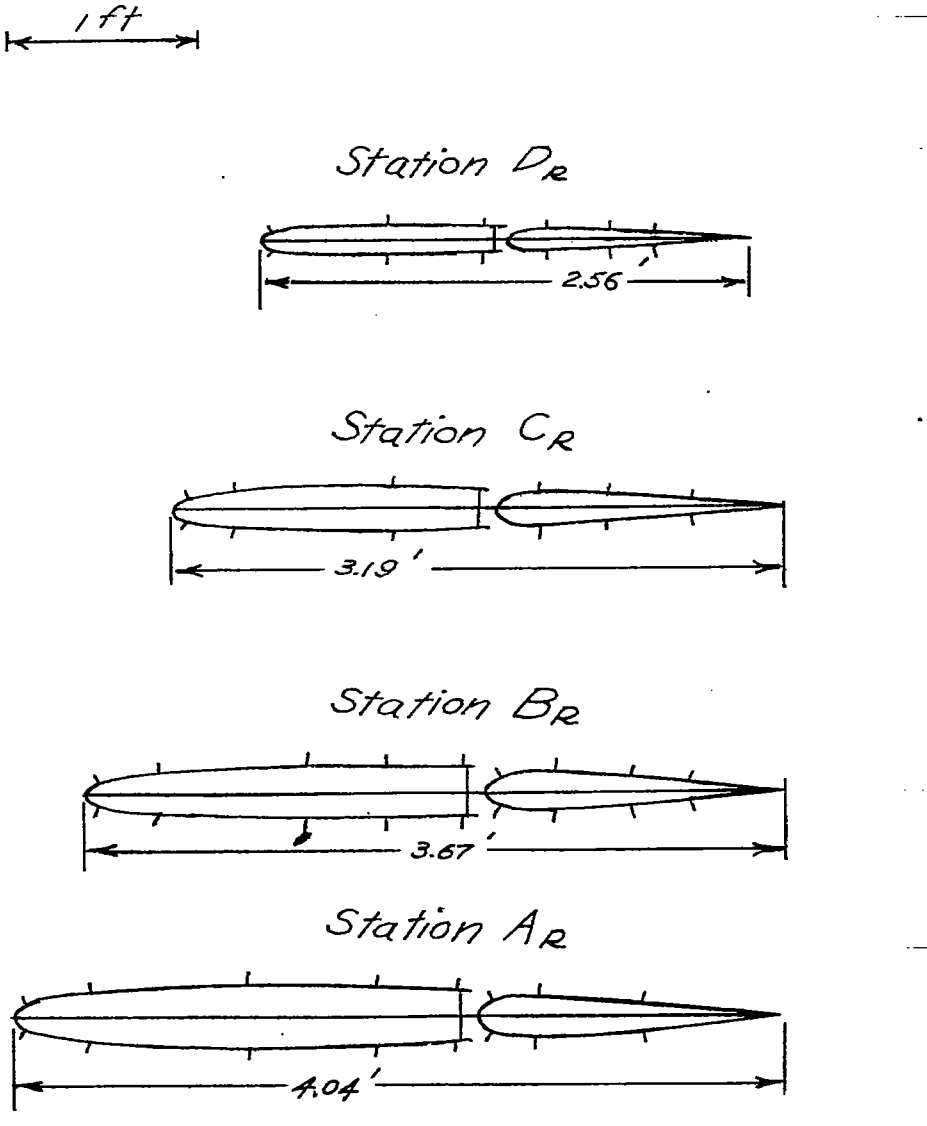

(b) Right tail sections

Figure 4. Continued. Test airplane.

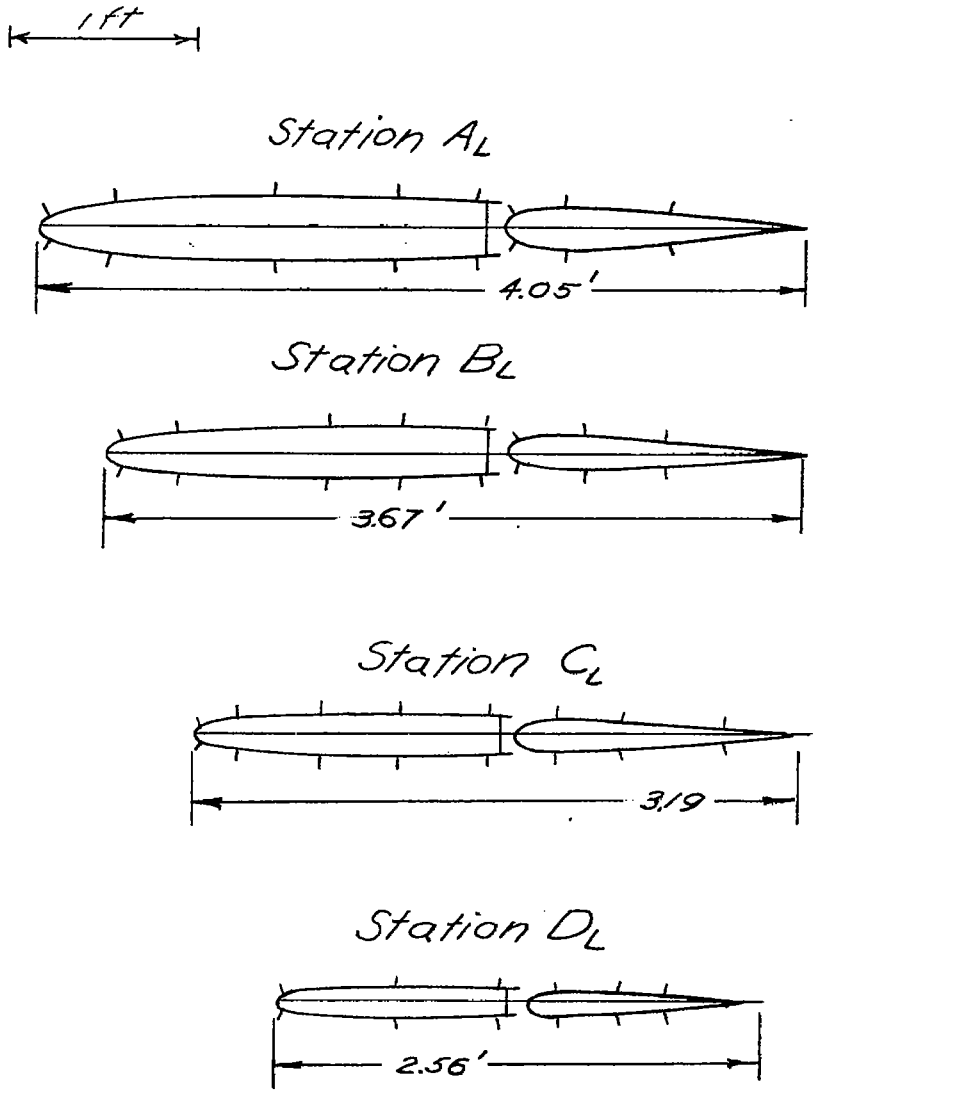

(c) Left tail sections.

Figure 4. - Concluded. Test airplane.

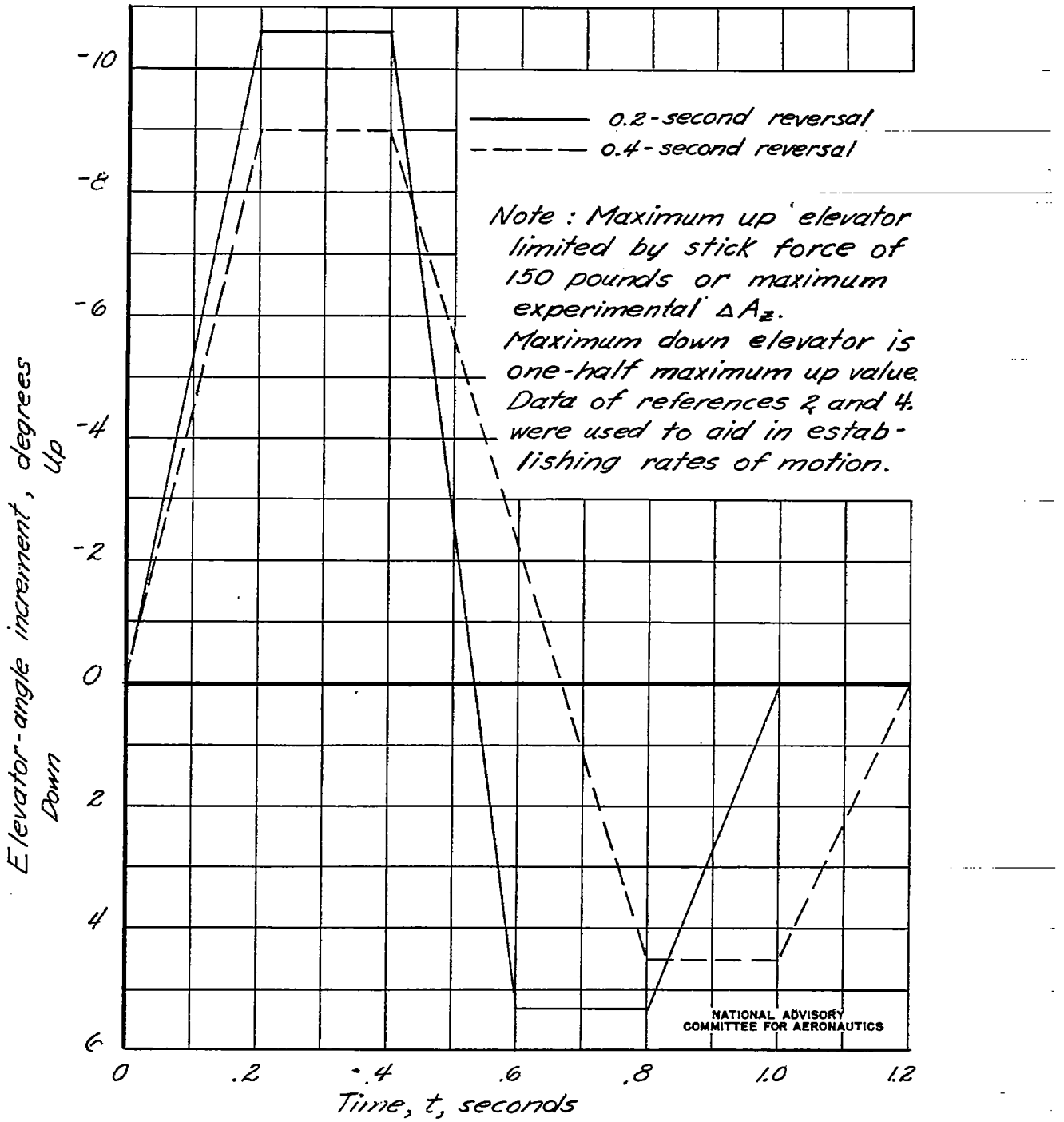

Figure 5. — Typical computed linear elevator motions used to determine the maneuvering tail-load increments by the tabular method.

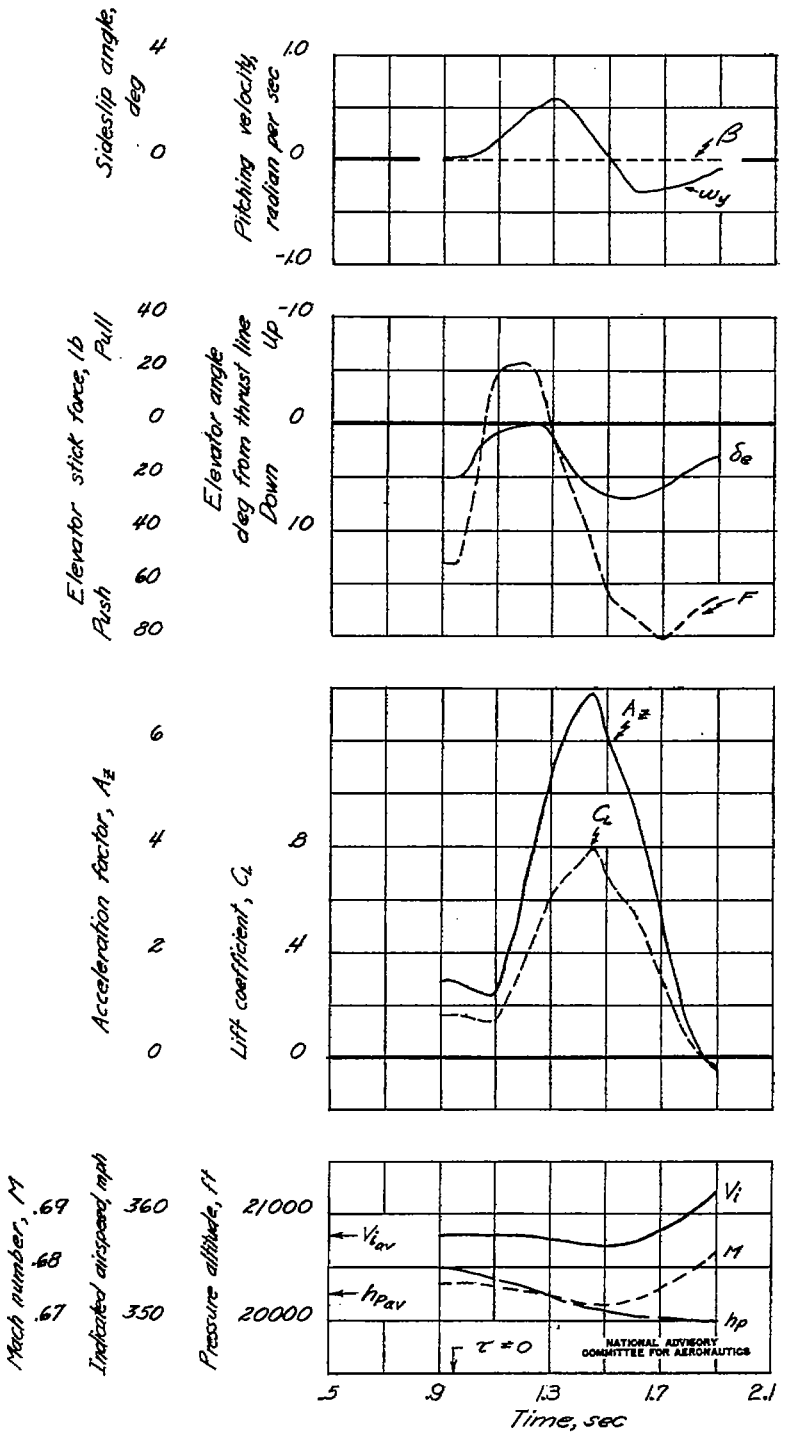

(a) Run 1.

Figure 6. — Time histories of basic flight data.

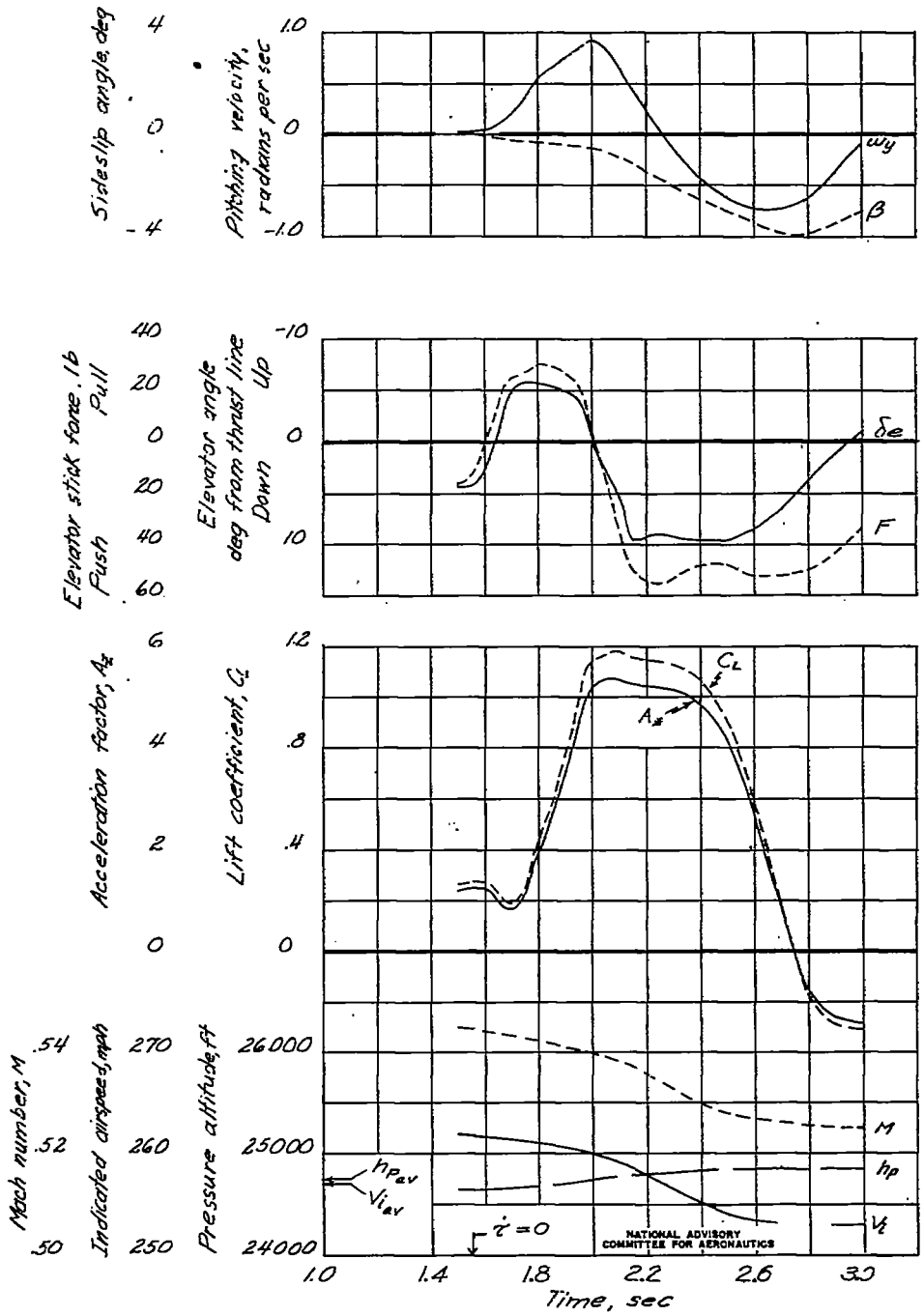

(b) Run 2.

Figure 6. — Continued.

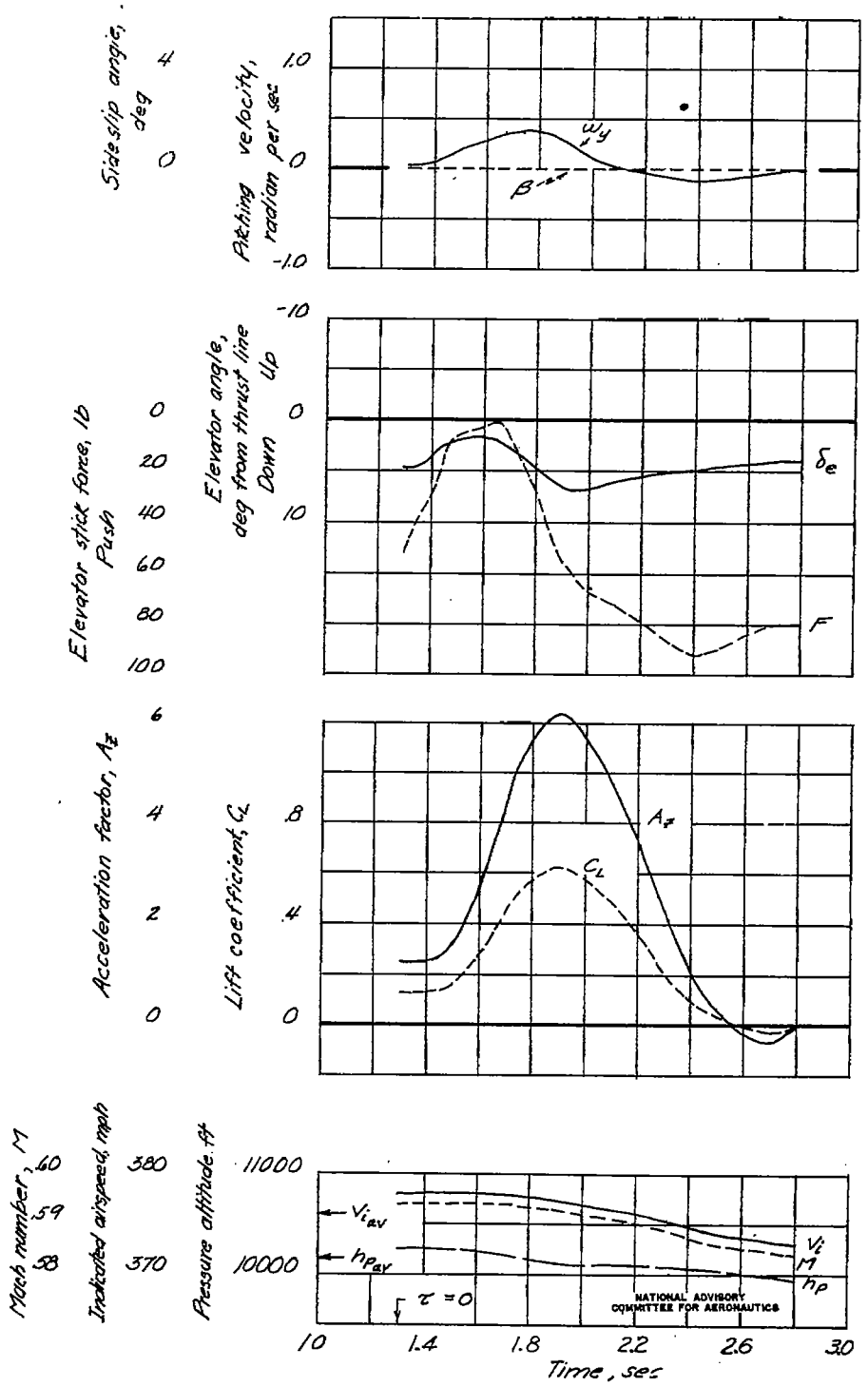

(c) Run 3.

Figure 6. — Continued.

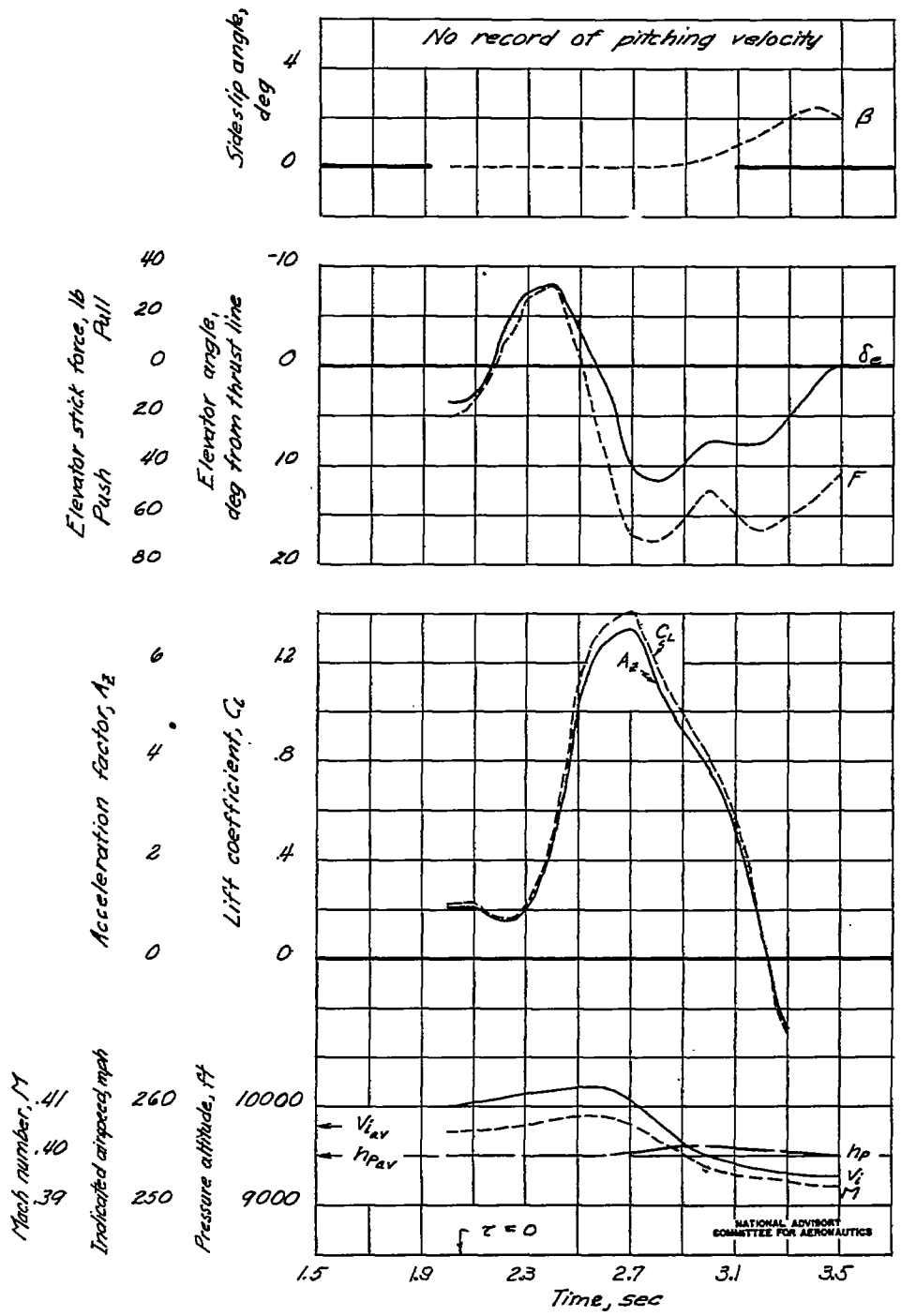

(d) Run 4.

Figure 6.- Continued.

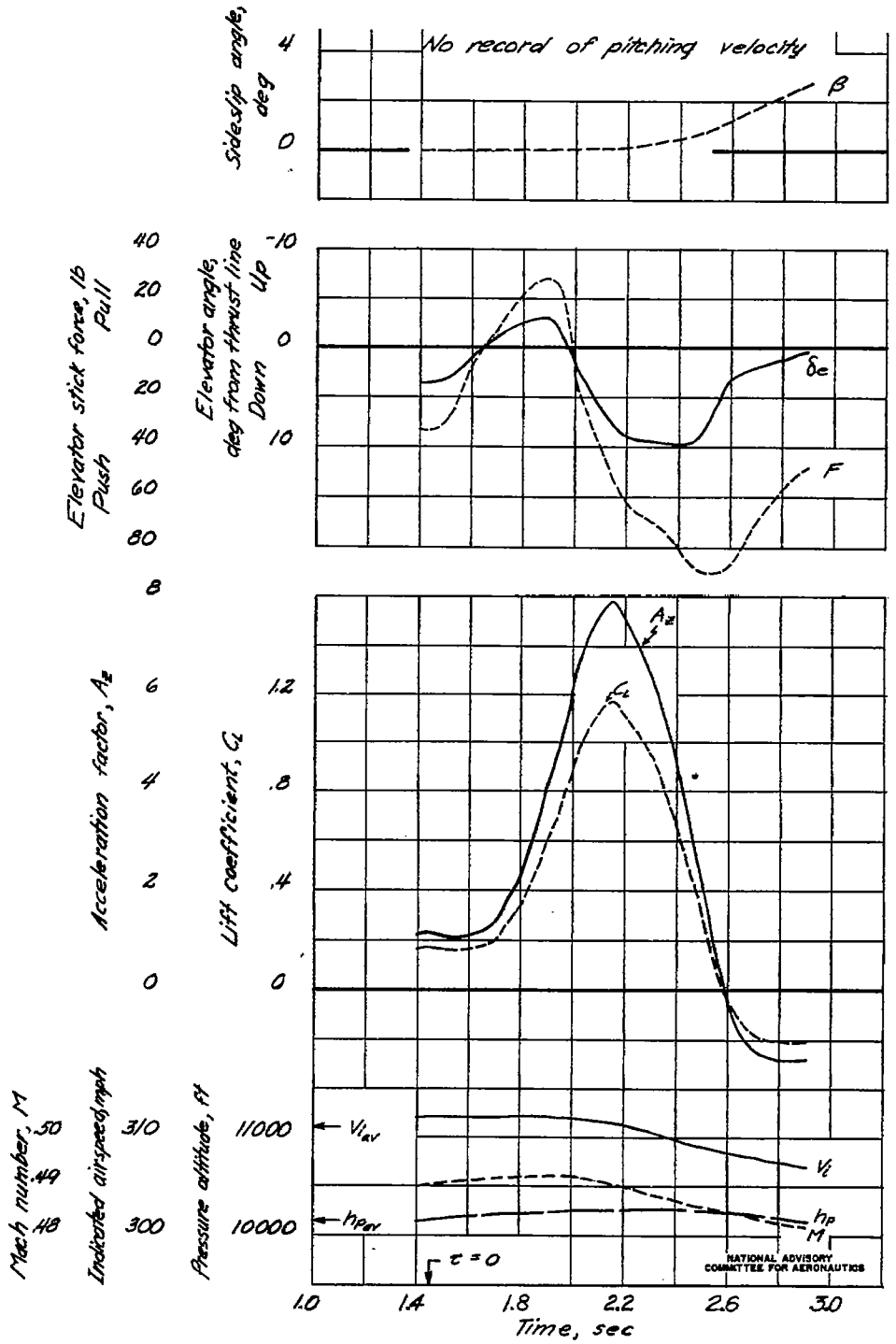

(e) Run 5.

Figure 6. – Continued

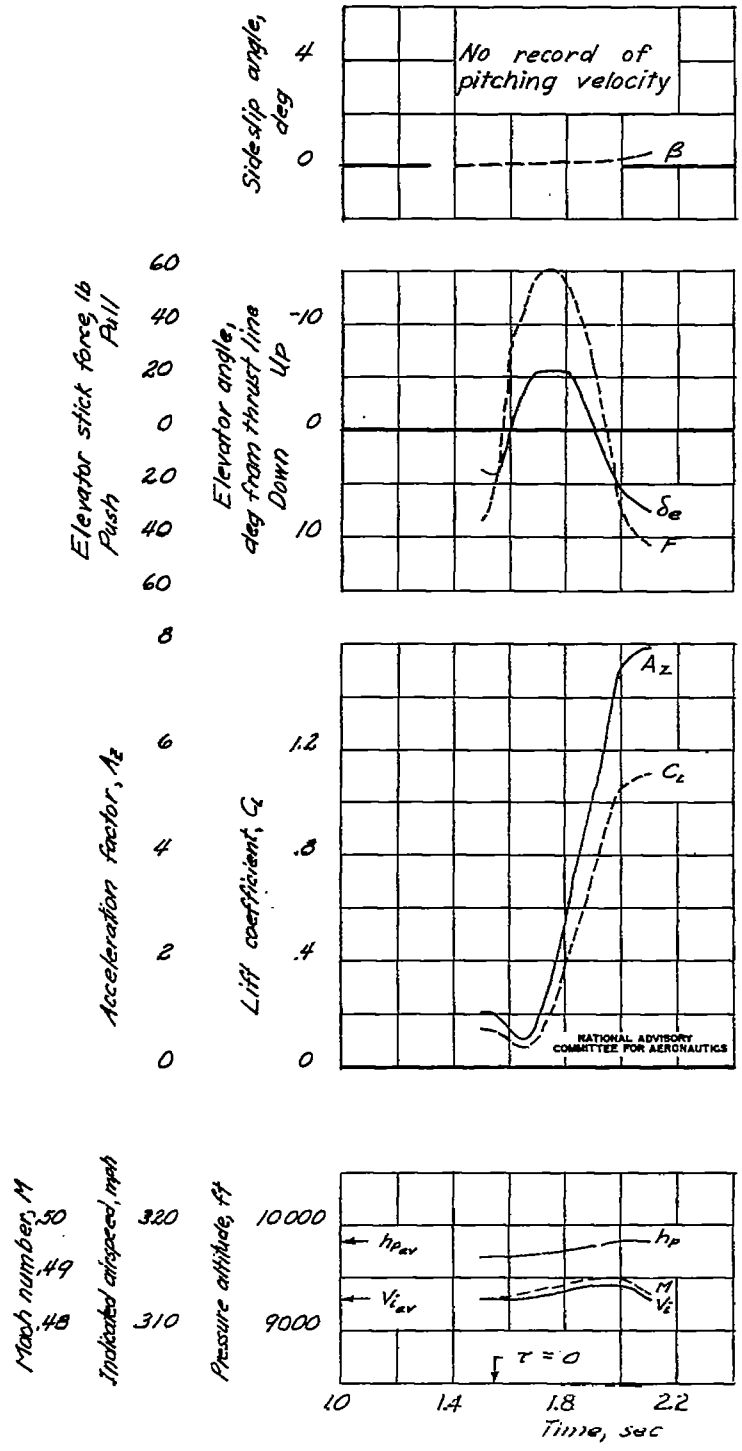

(f) Run 6

Figure 6.- Concluded.

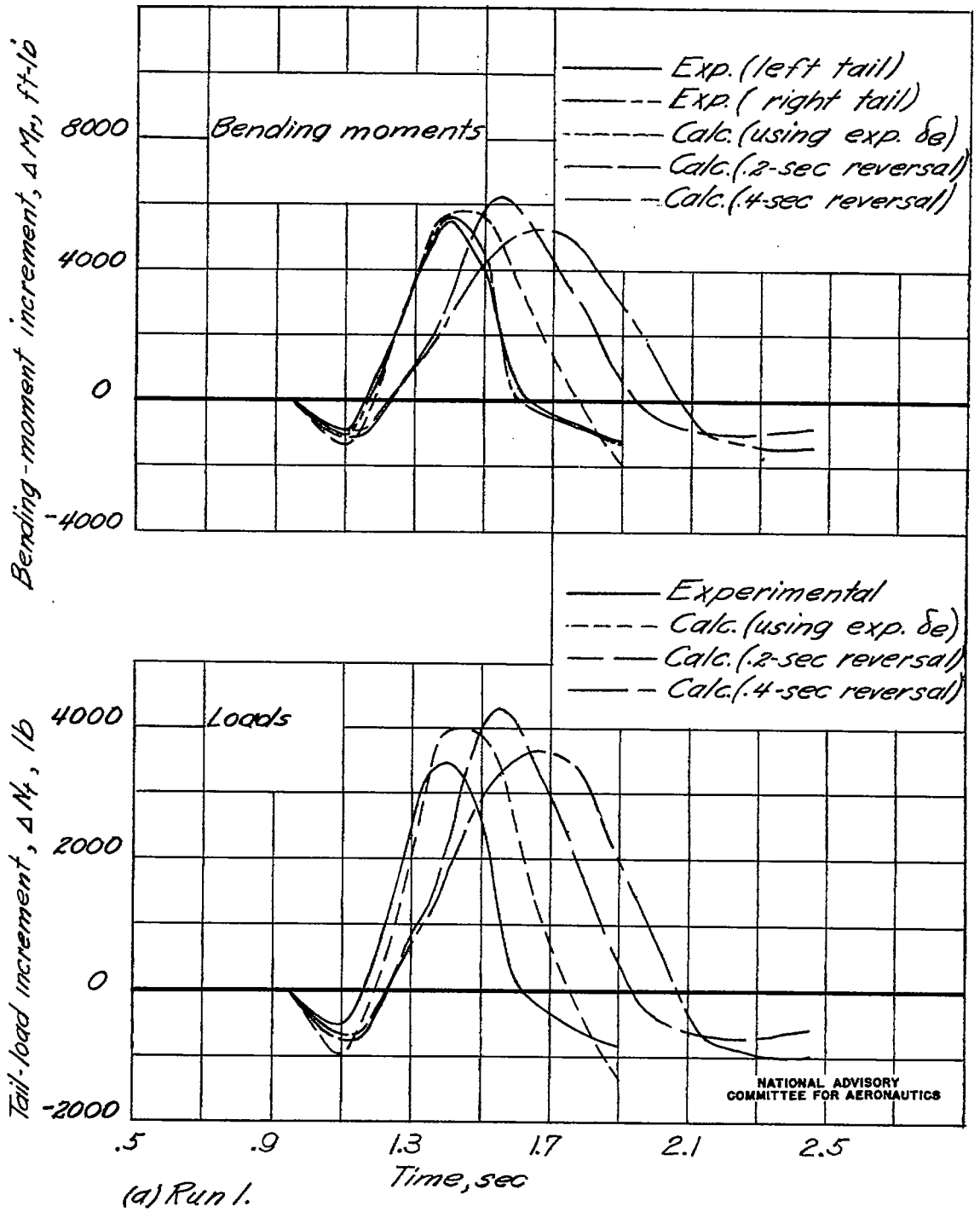

Figure 7. — Comparison between measured and calculated tail-load and bending-moment increments.

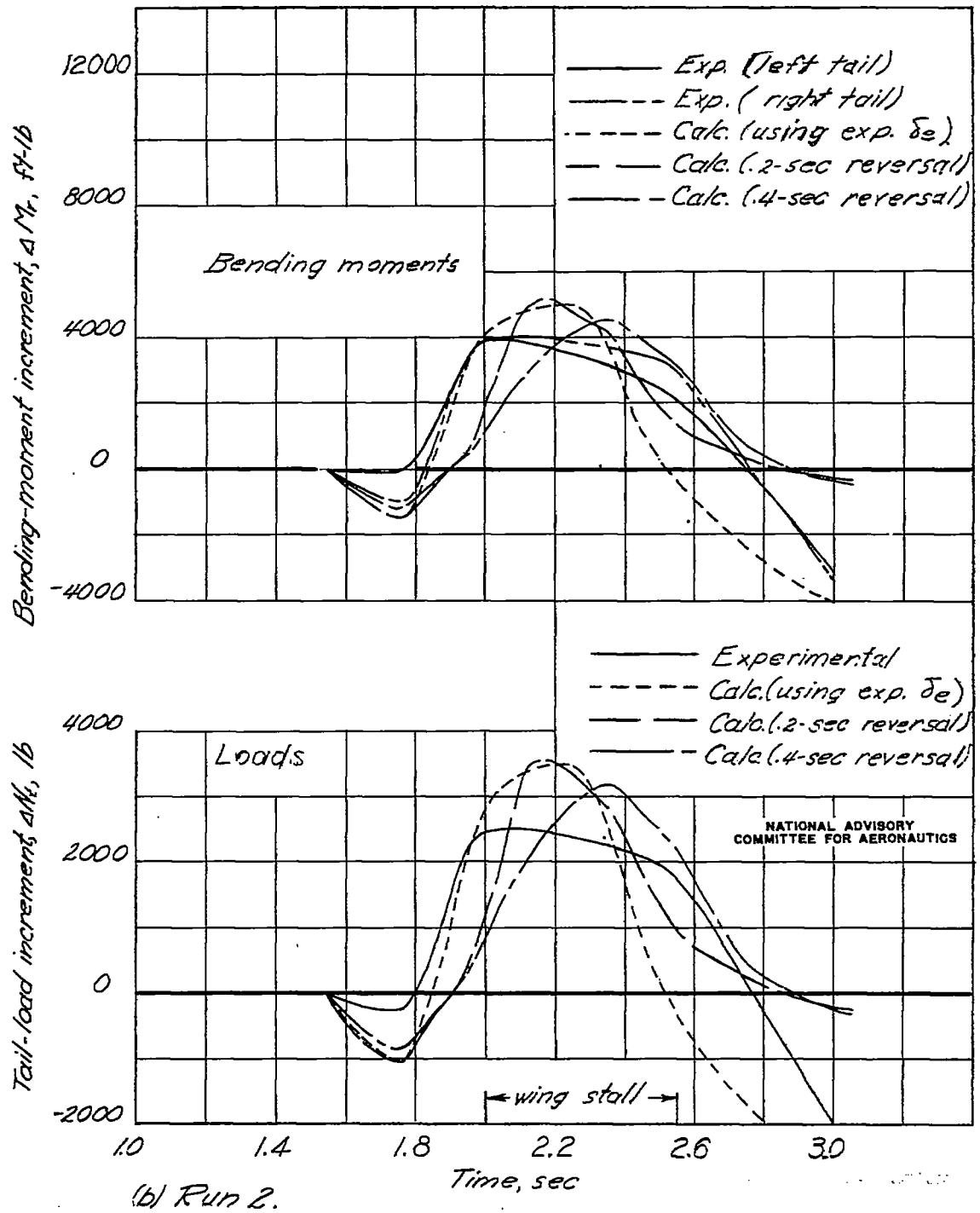

(b) Run 2.

Figure 7. — Continued.

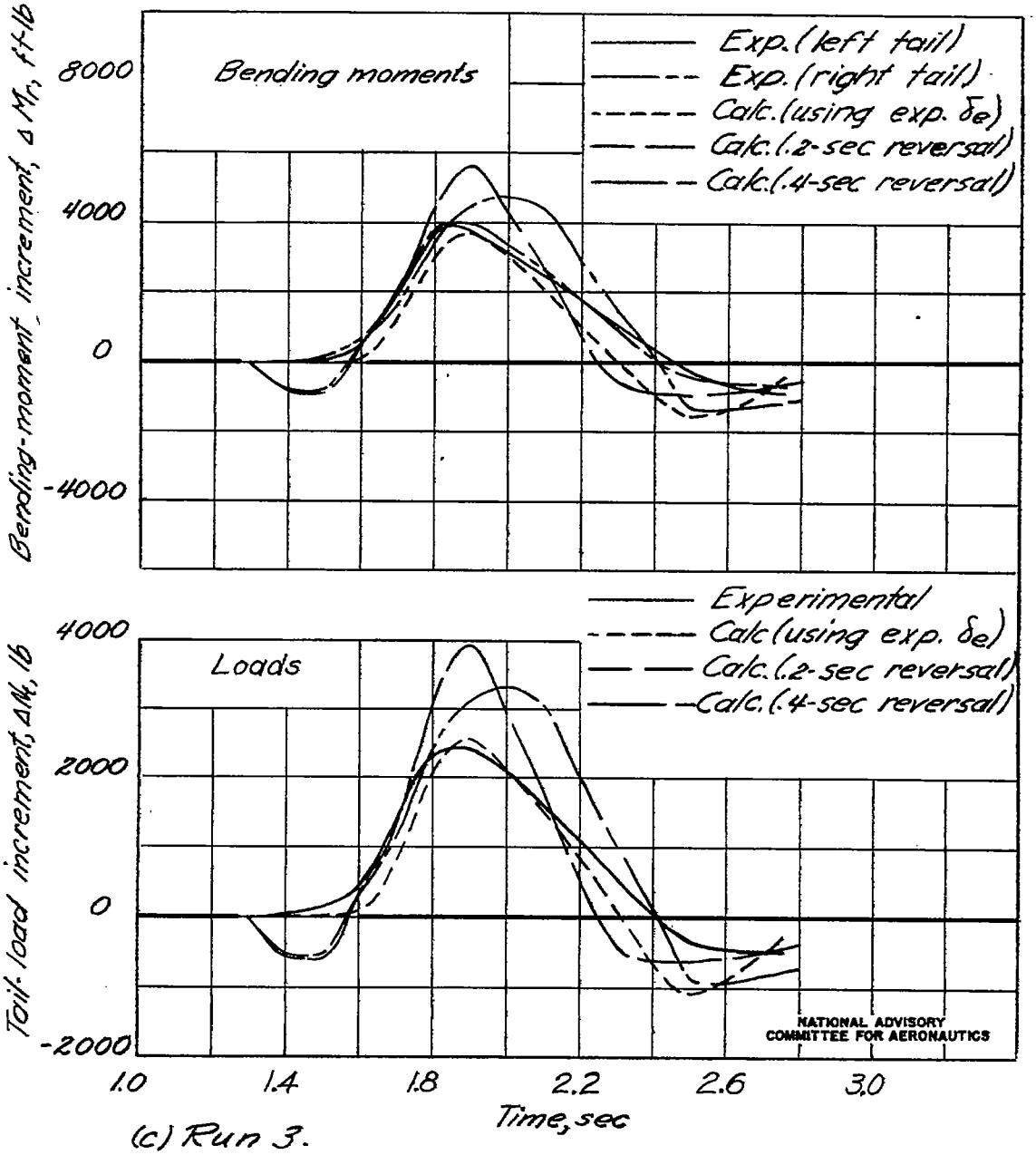

(c) Run 3.

Figure 7. — Continued.

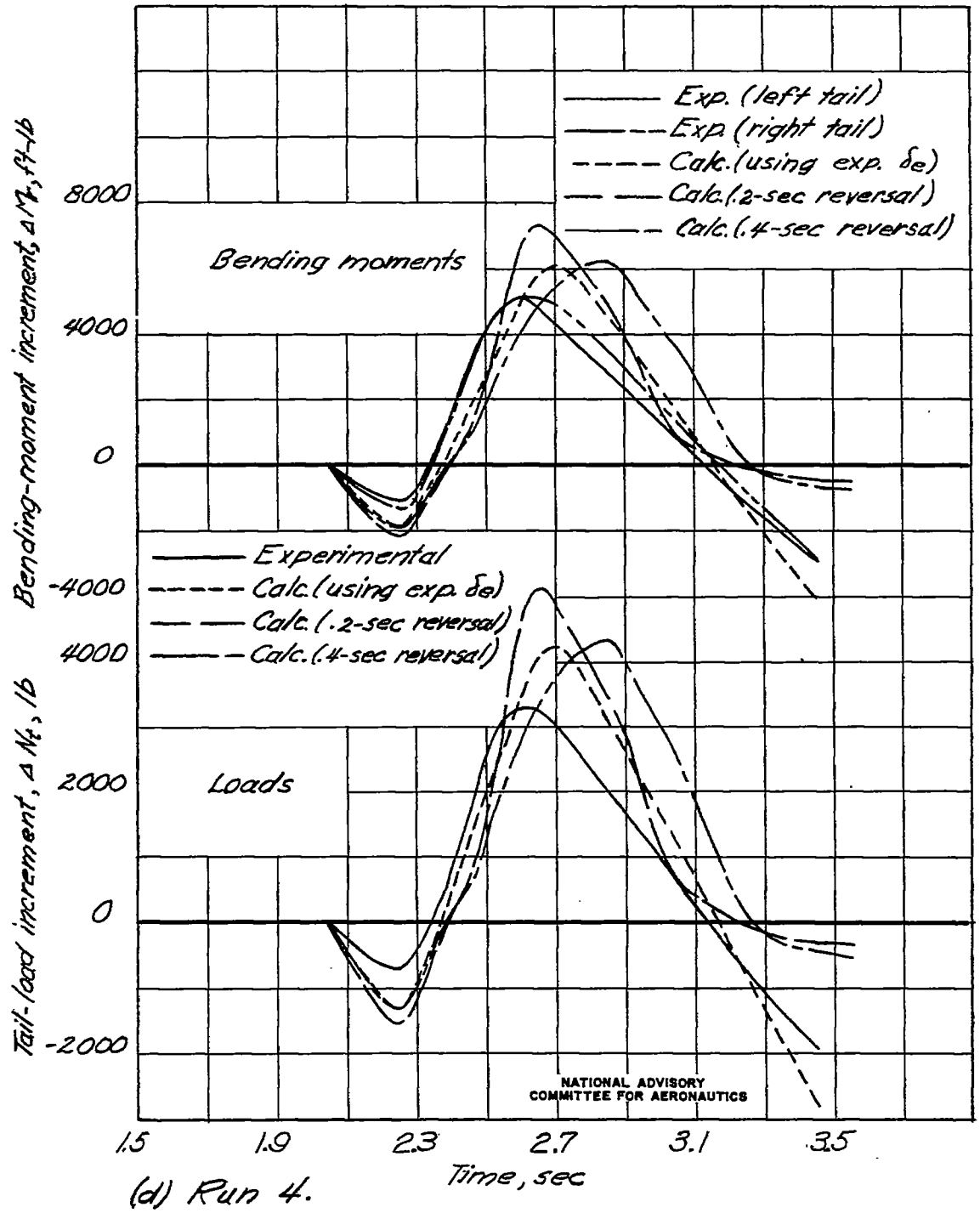

(d) Run 4.

Figure 7. – Continued.

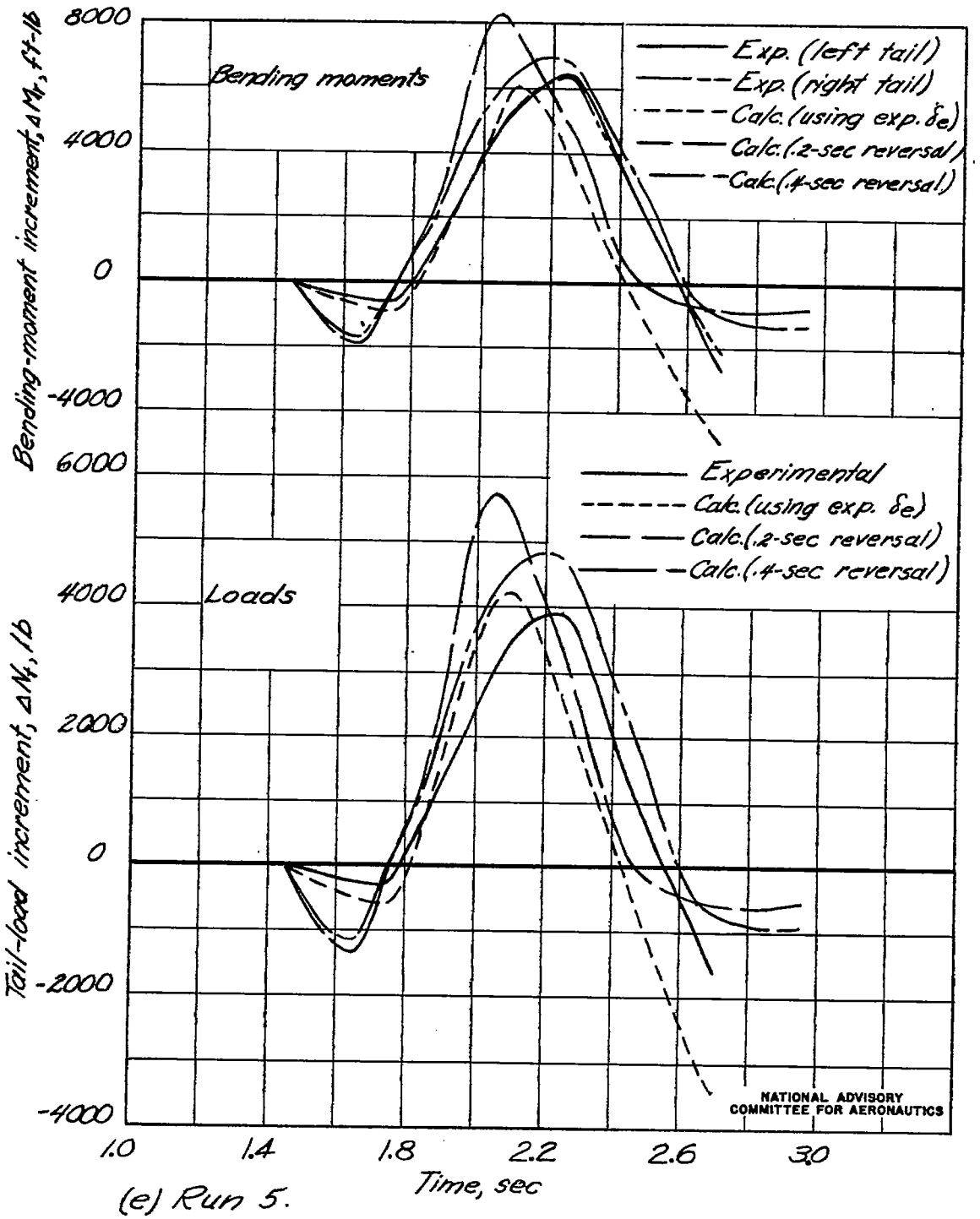

(e) Run 5.

Figure 7.- Continued.

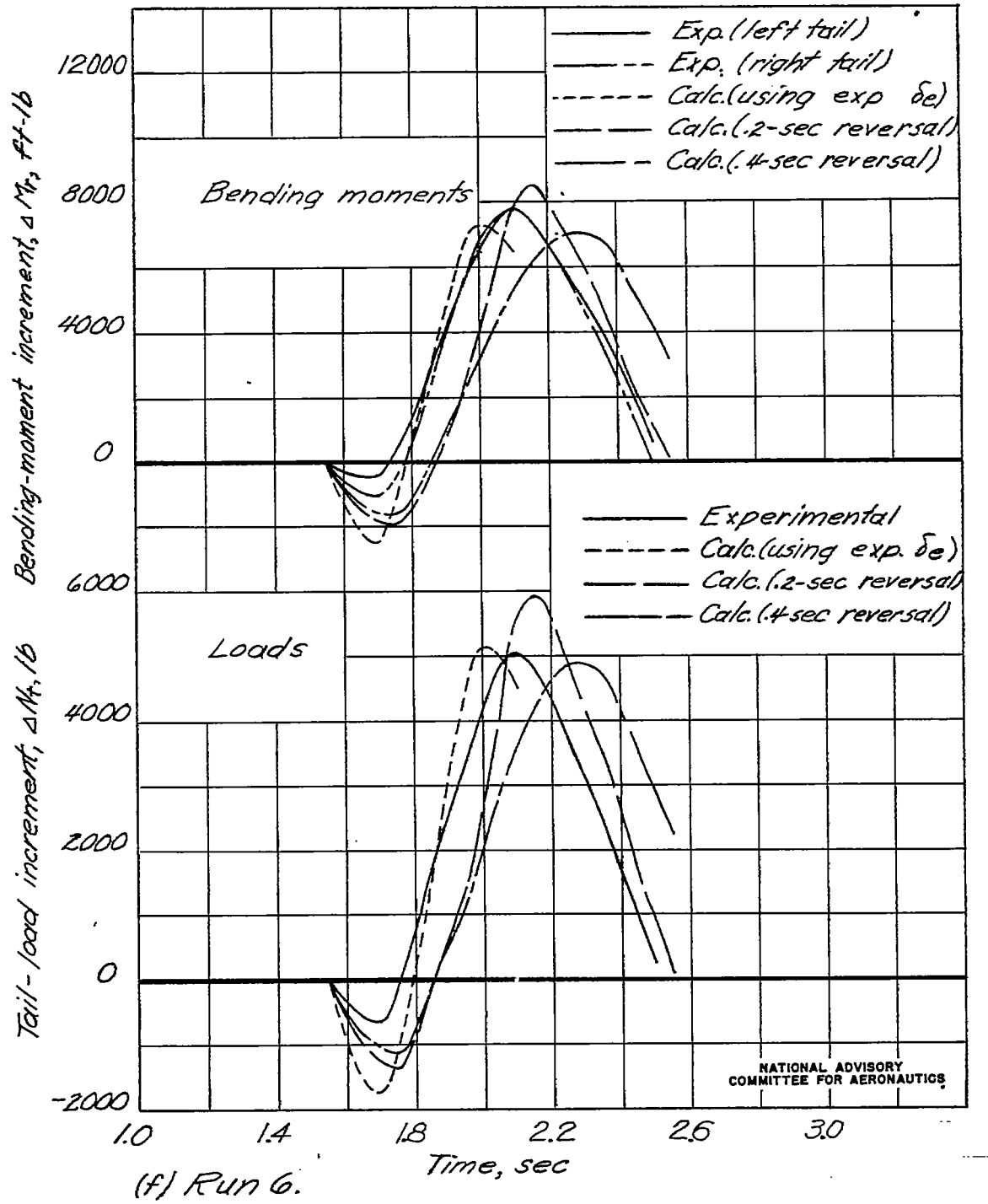

(f) Run 6.

Figure 7. — Concluded.

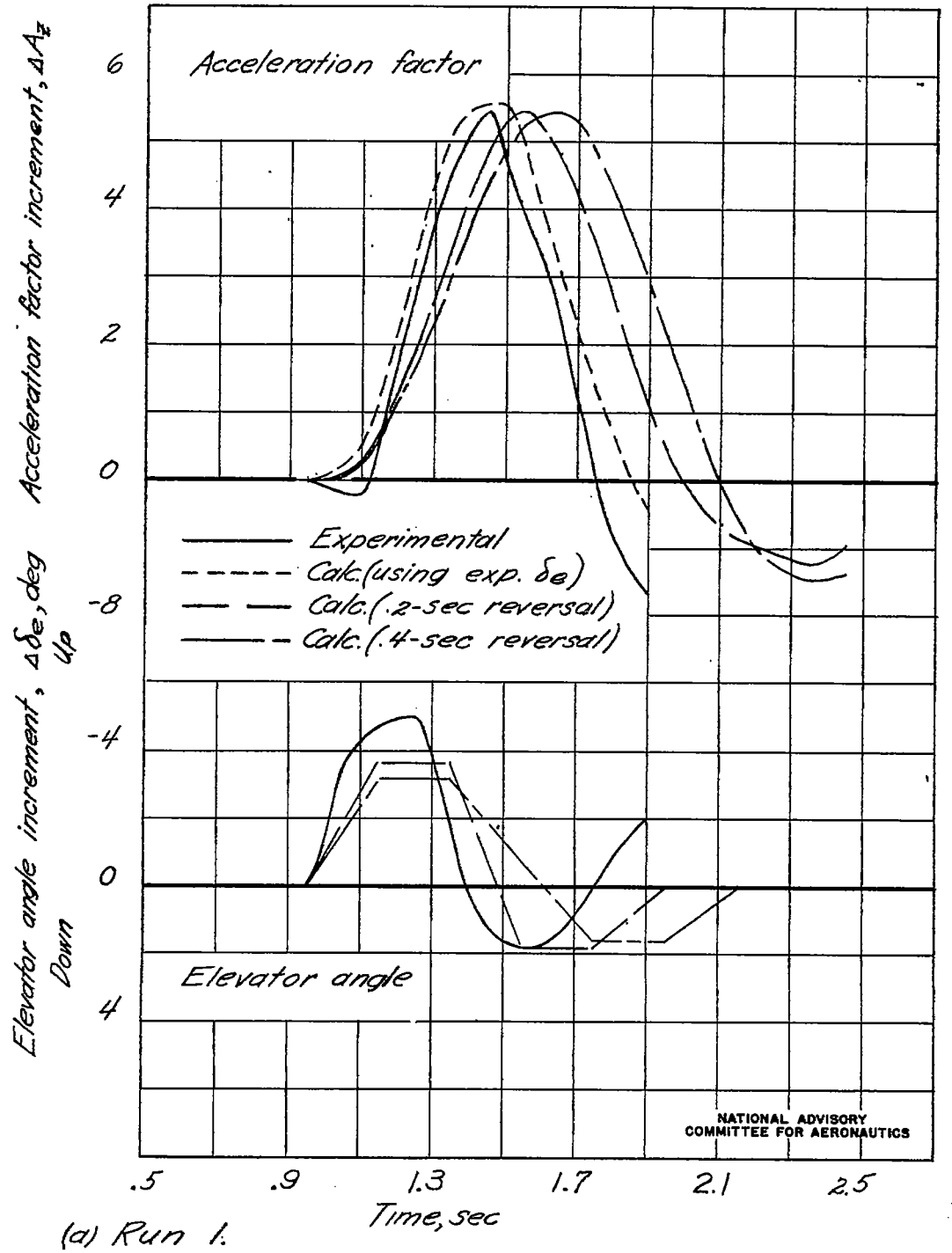

(a) Run 1.

Figure 8.— Comparison between measured and calculated elevator-angle and acceleration-factor increments.

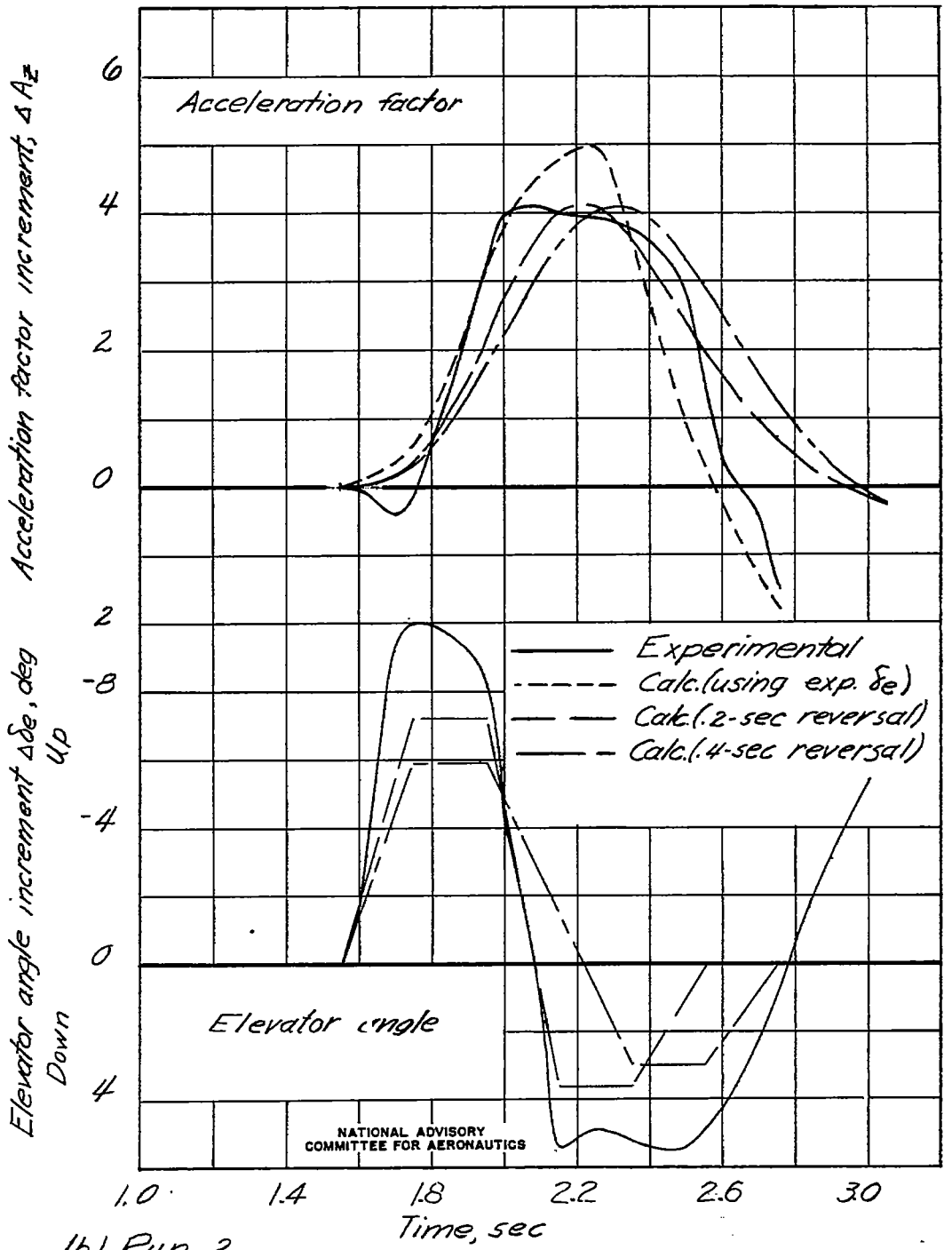

(b) Run 2.

Figure 8. — Continued.

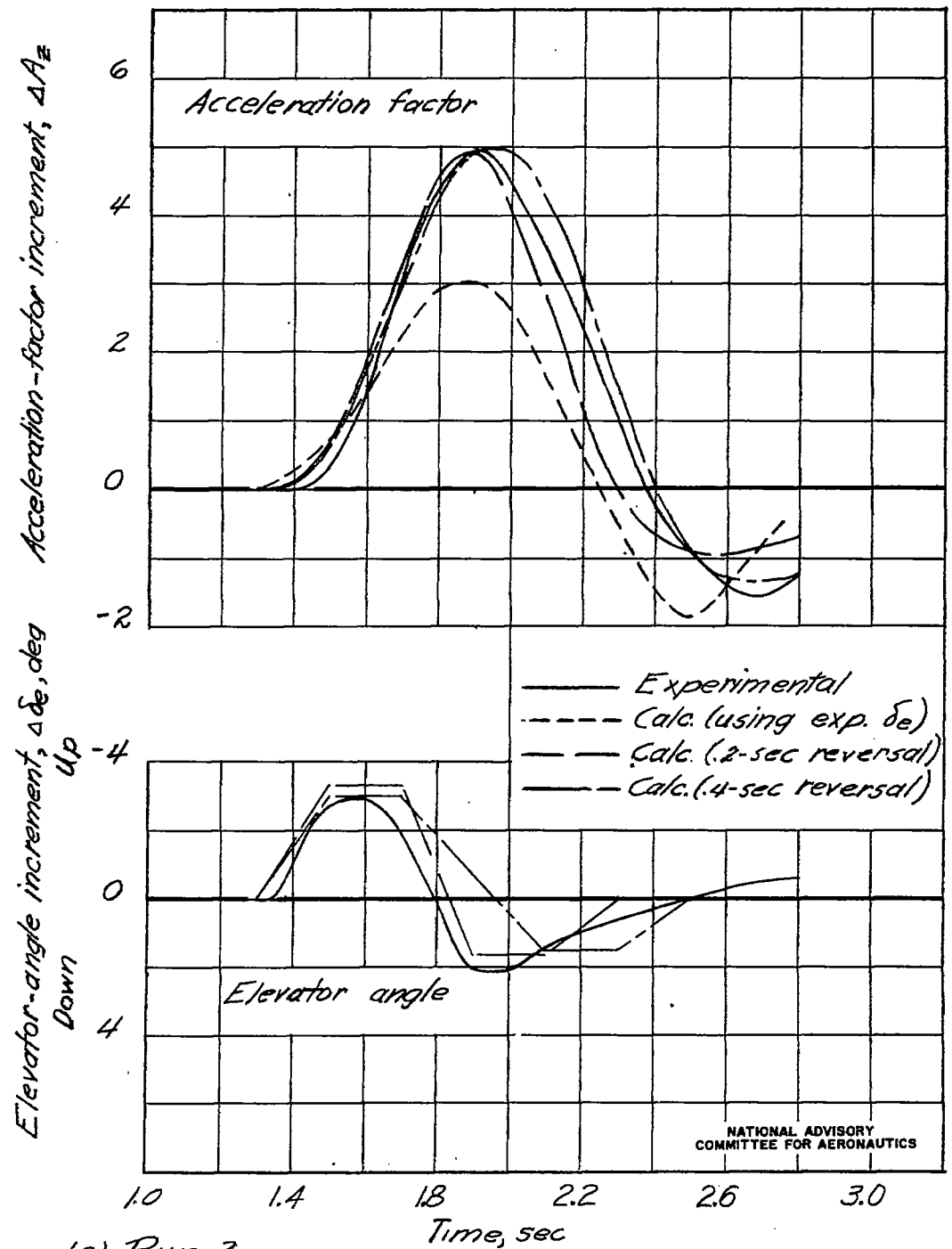

(c) Run 3.

Figure 8. — Continued.

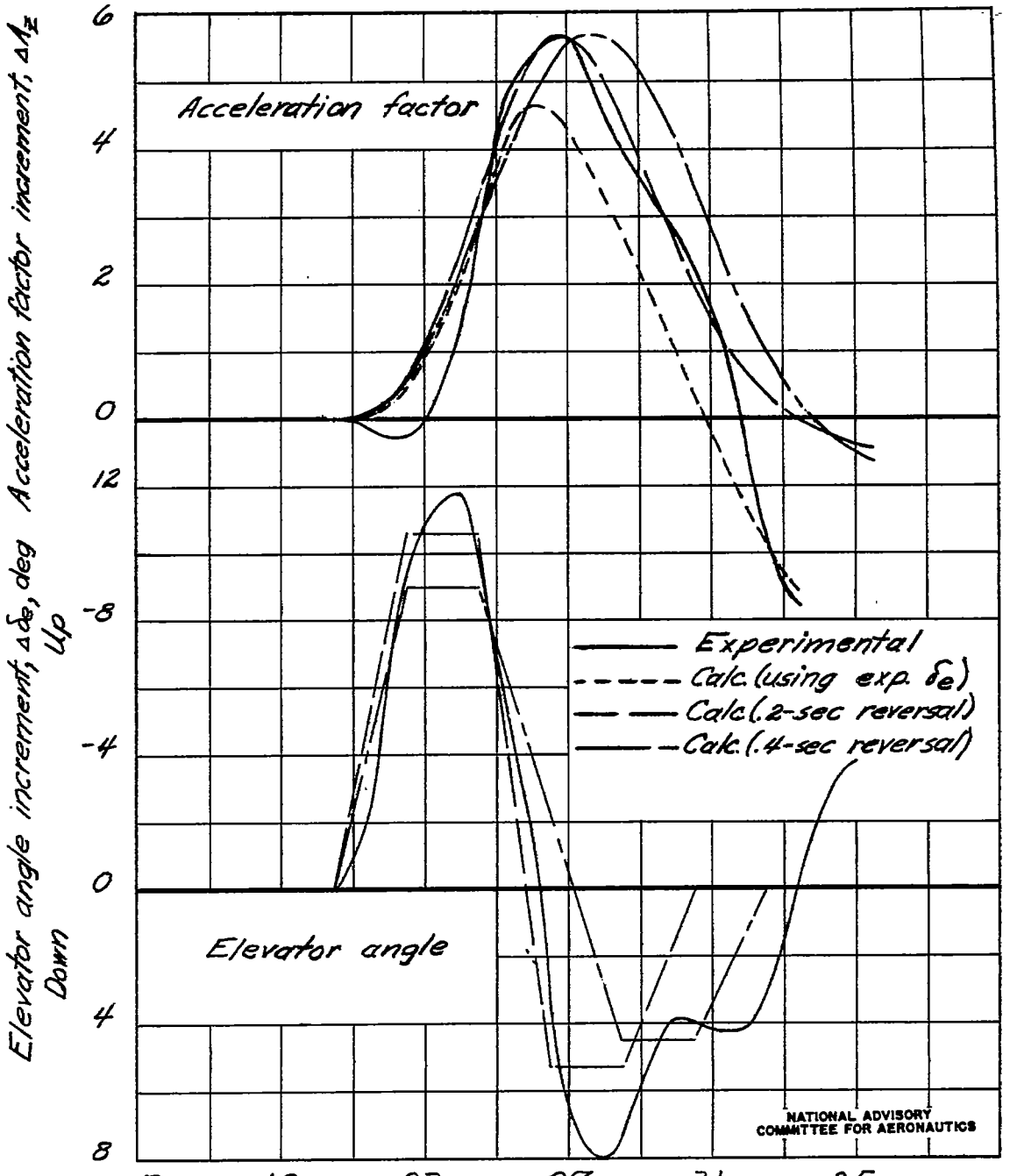

(d) Run 4.

Figure 8.– Continued.

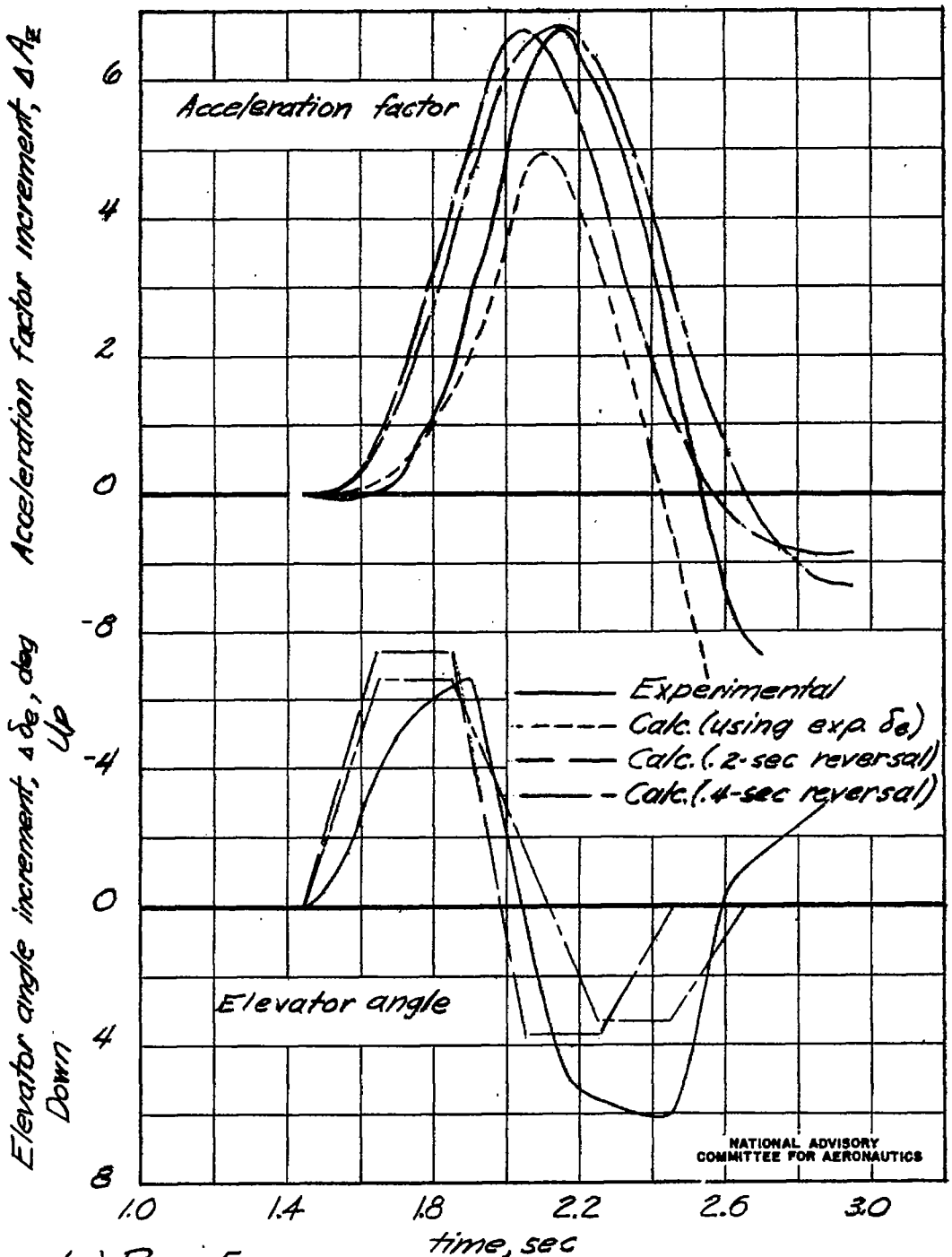

(e) Run 5.

Figure 8. — Continued.

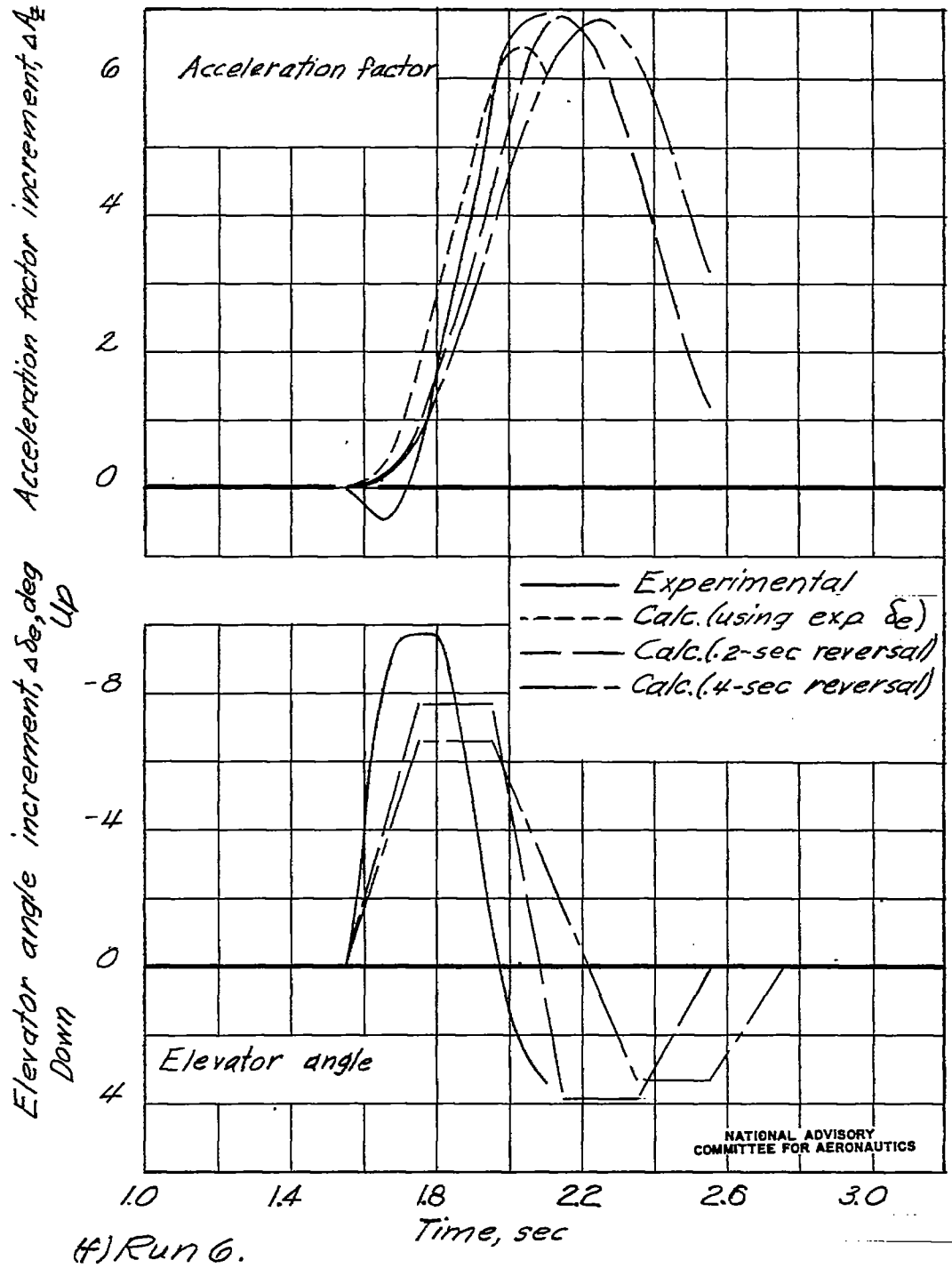

(f) Run 6.

Figure 8.— Concluded.

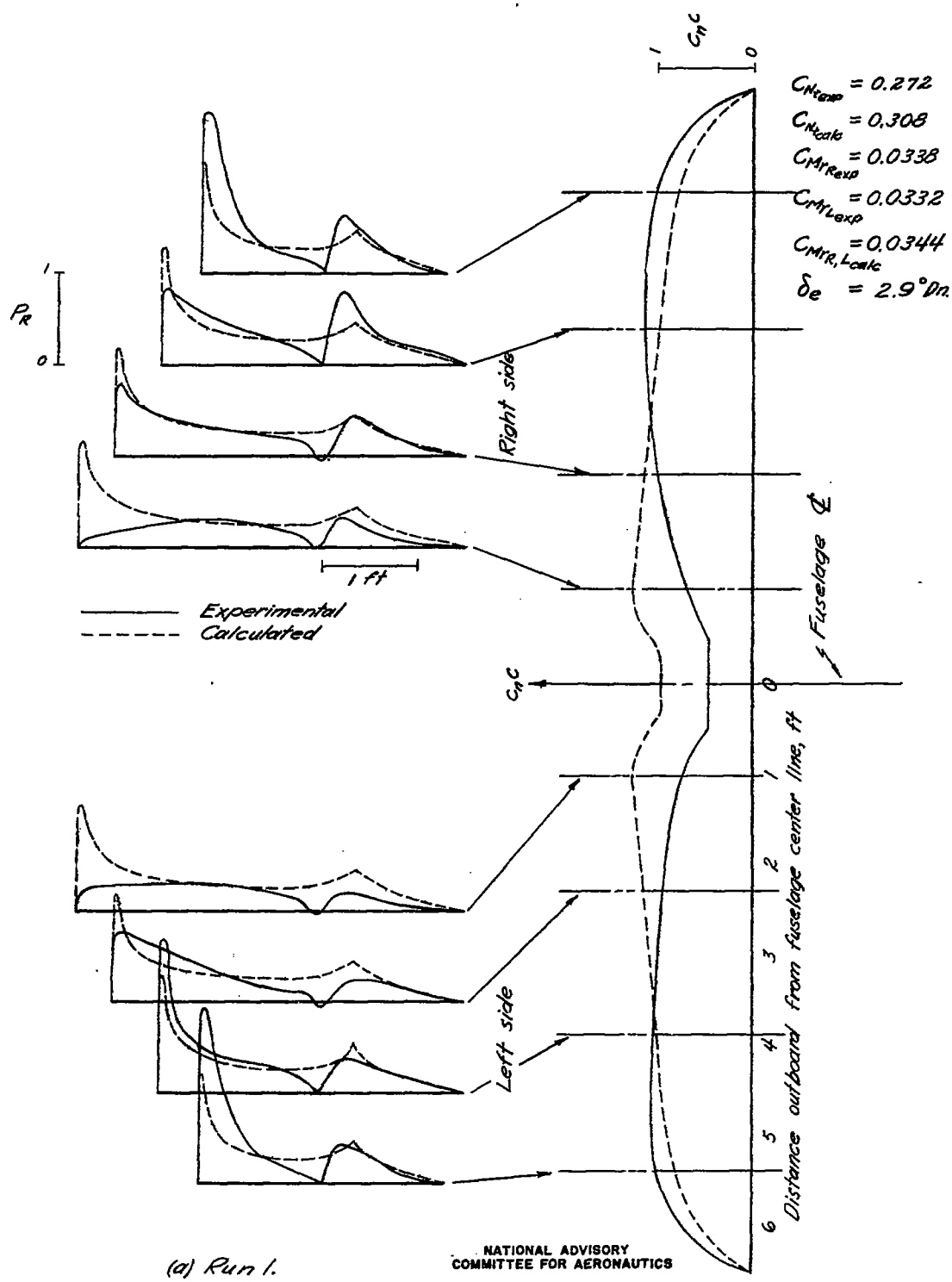

(a) Run 1.

Figure 9. – Comparison between measured and computed load distributions at times corresponding to the maximum calculated loads based on the experimental elevator motions. δ_e measured from stabilizer centerline.

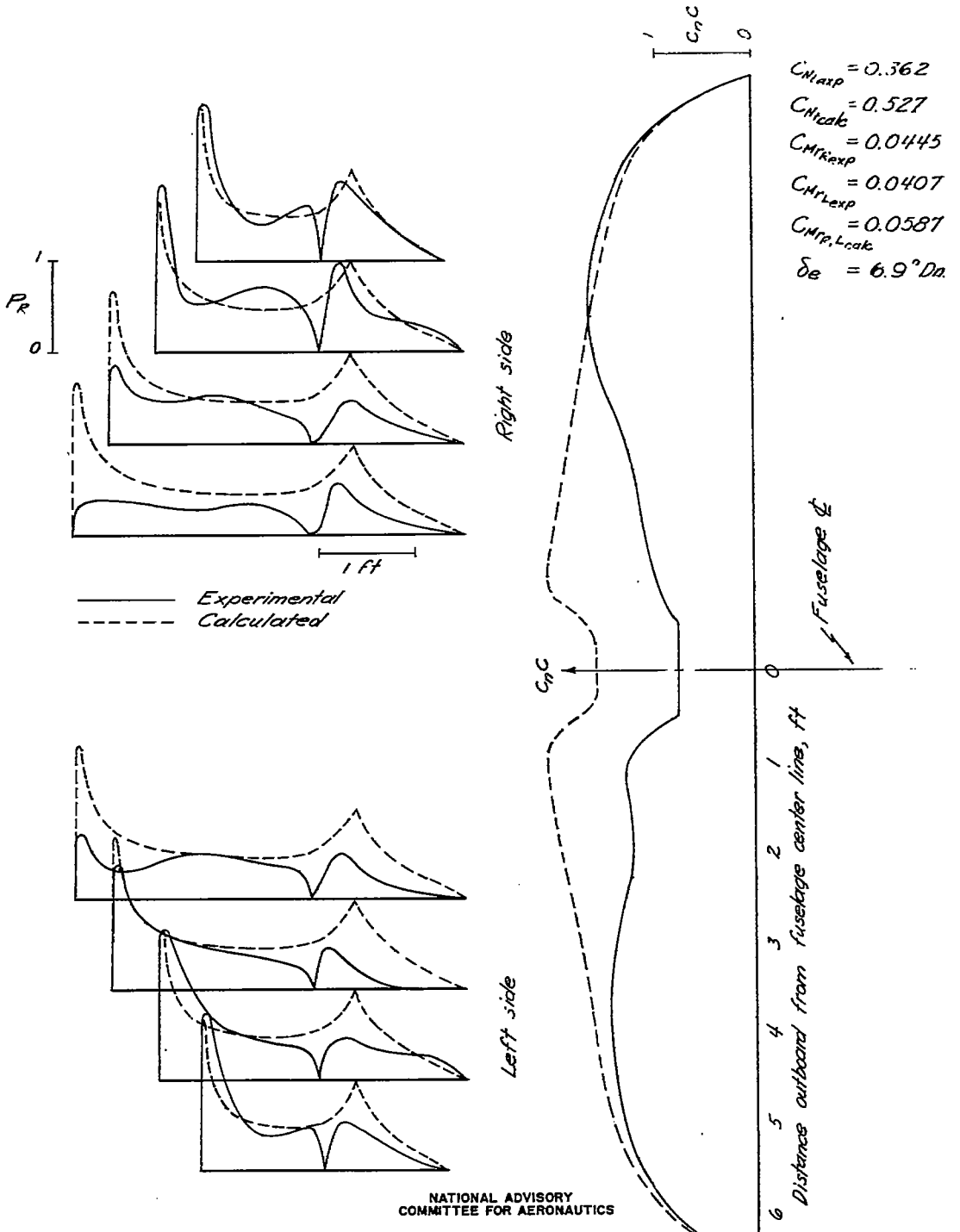

(b) Run 2.

Figure 9.– Continued.

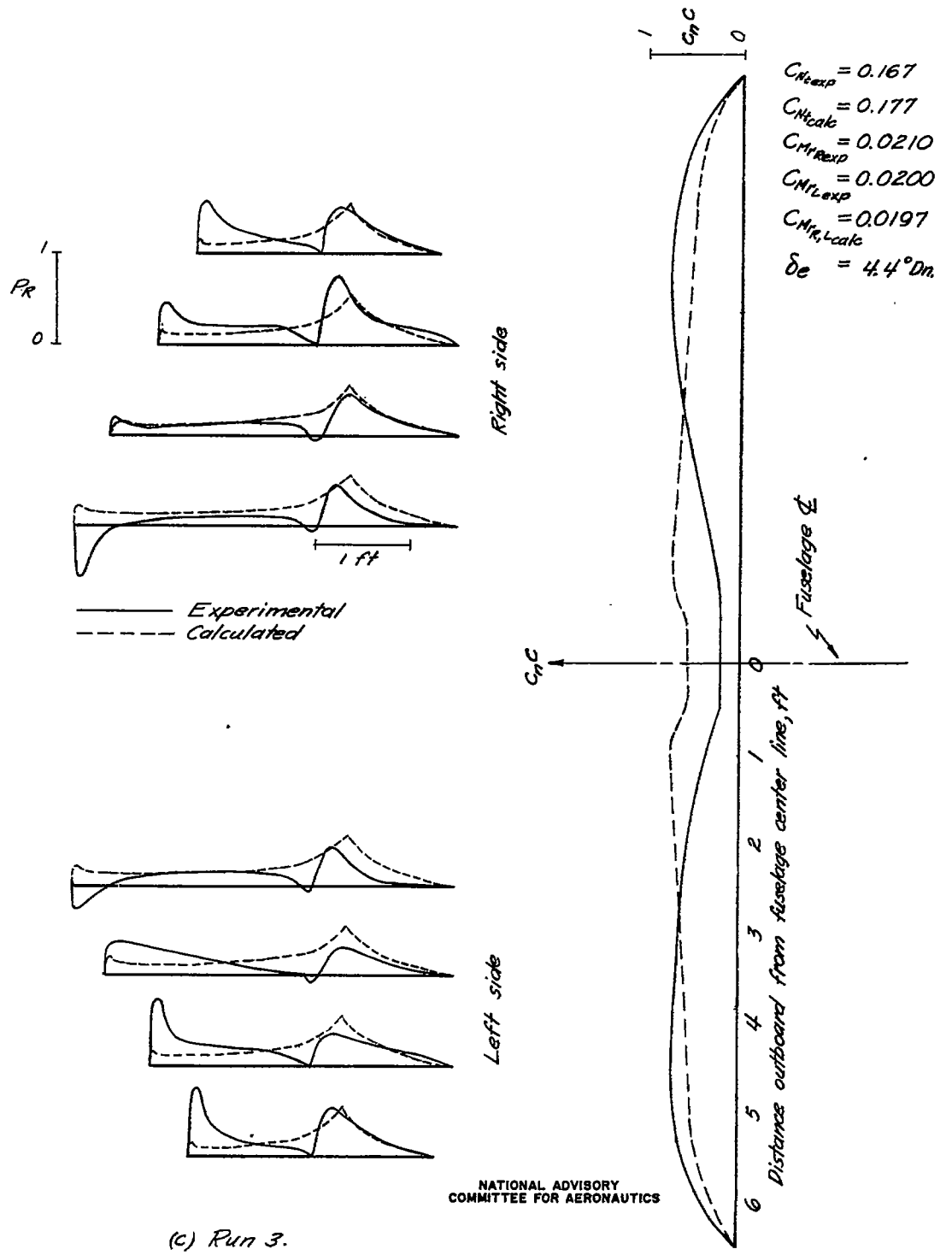

(c) Run 3.

Figure 9. - Continued

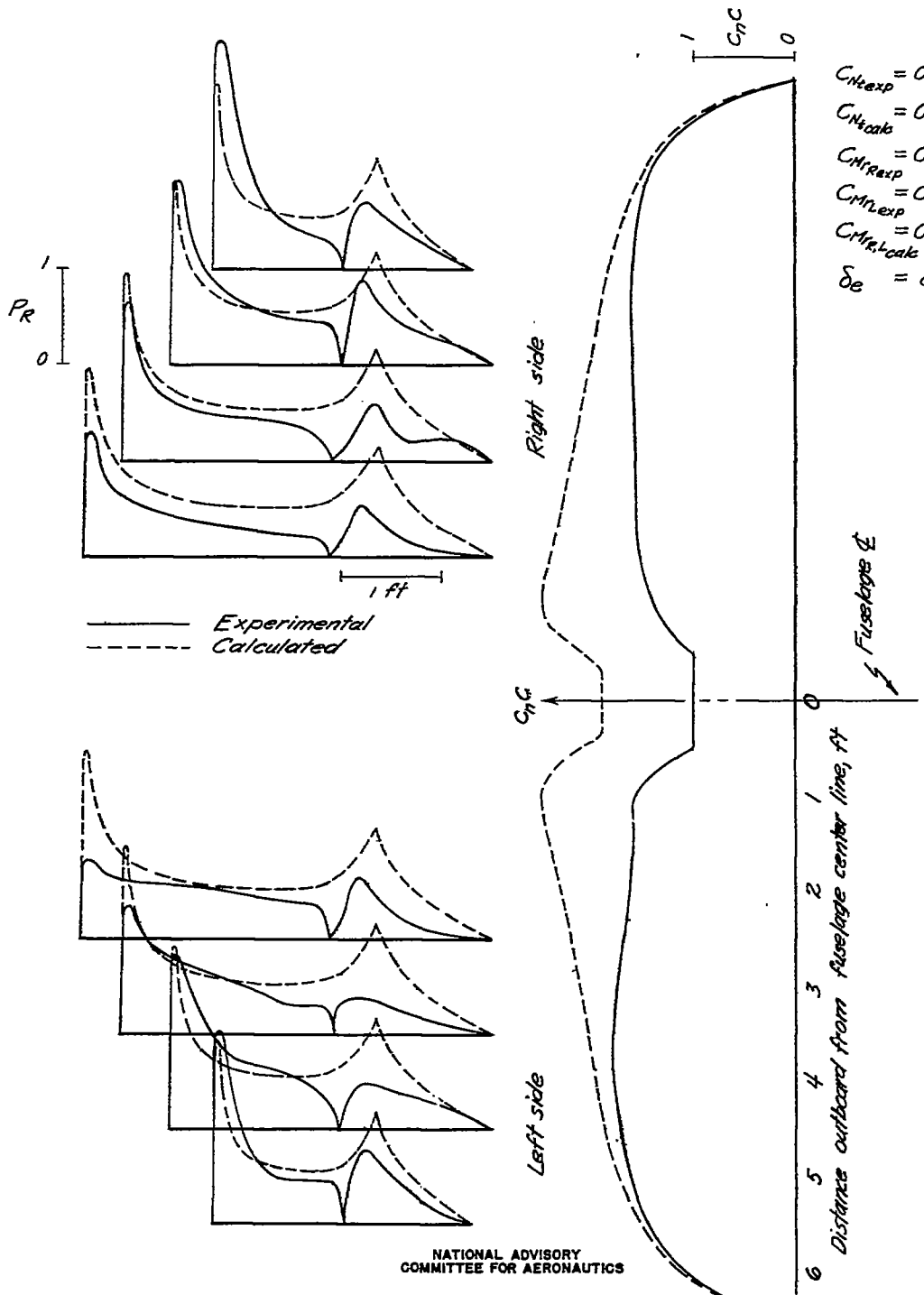

(d) Run 4.

Figure 9.- Continued.

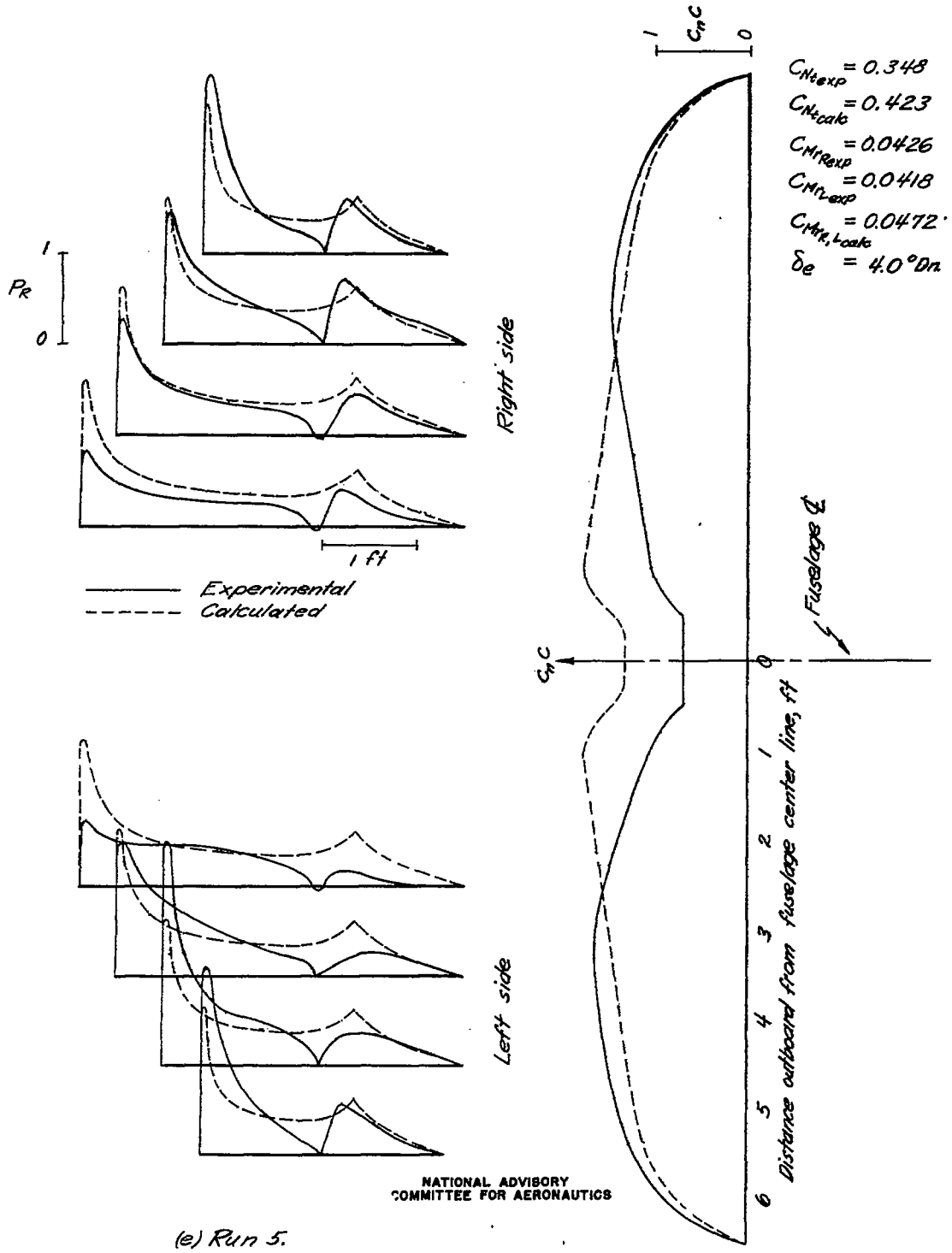

(e) Run 5.

Figure 9. — Continued.

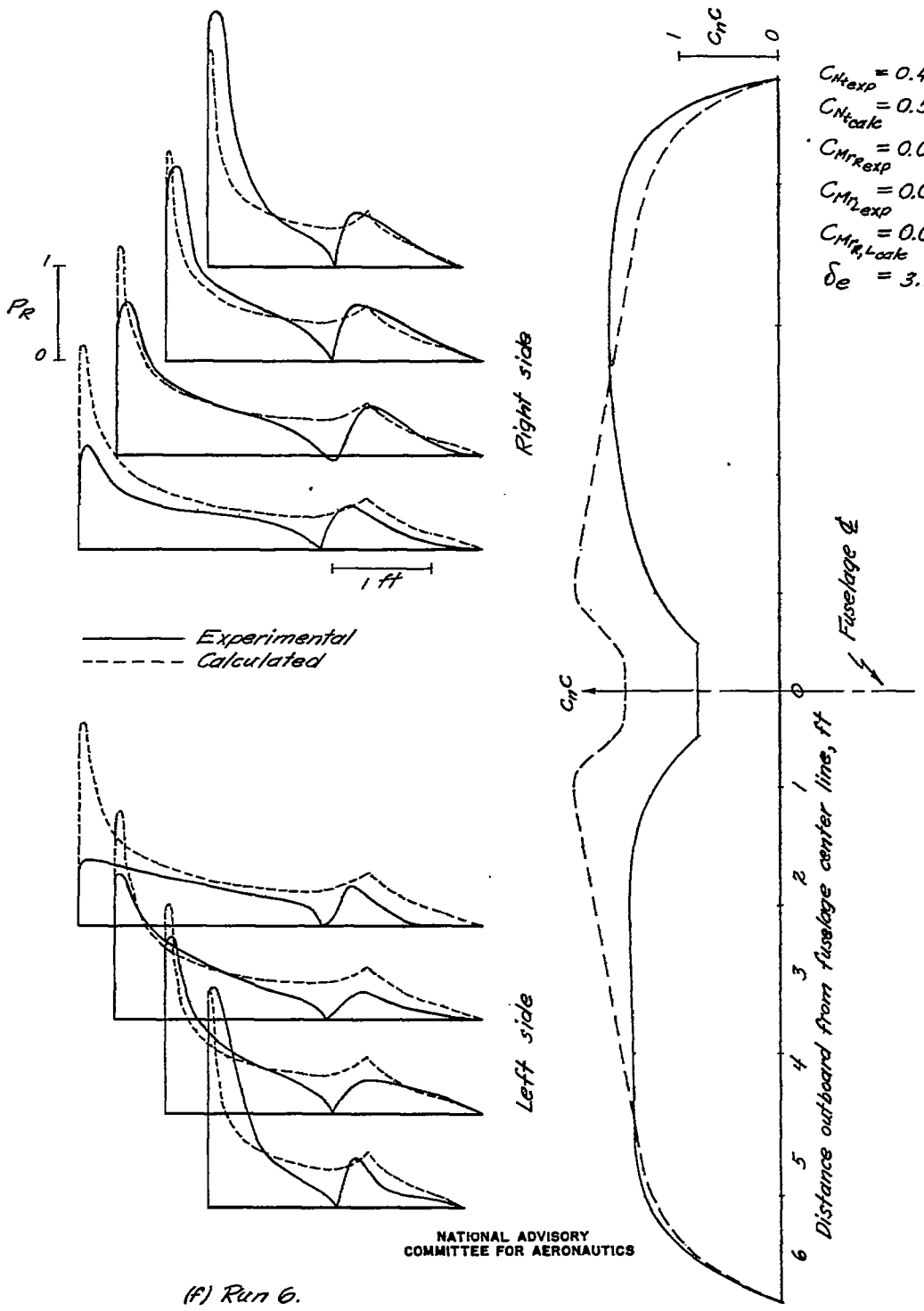

(f) Run 6.

Figure 9. – Concluded.

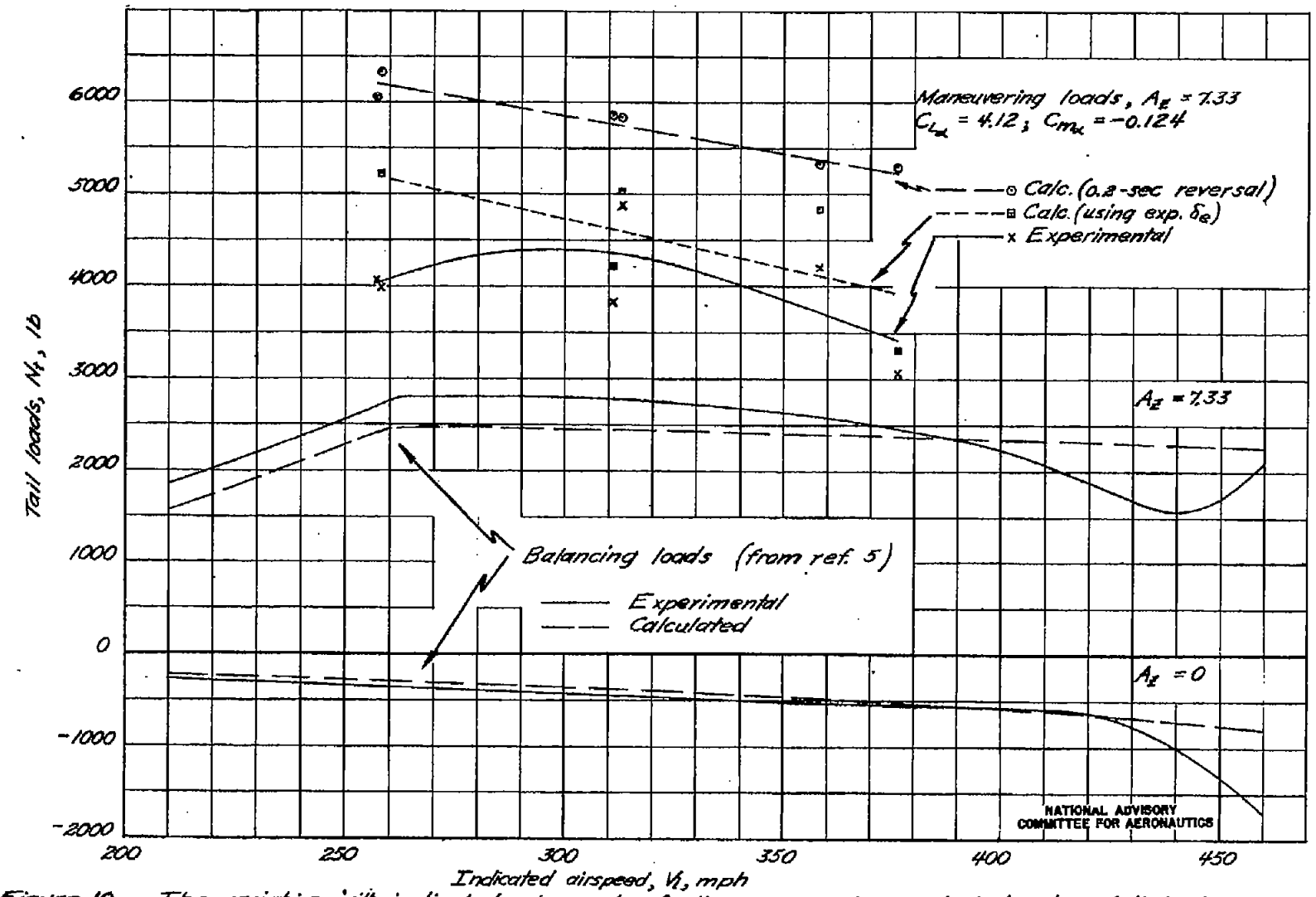

Figure 10.— The variation with indicated airspeed of the maneuvering and balancing tail loads.

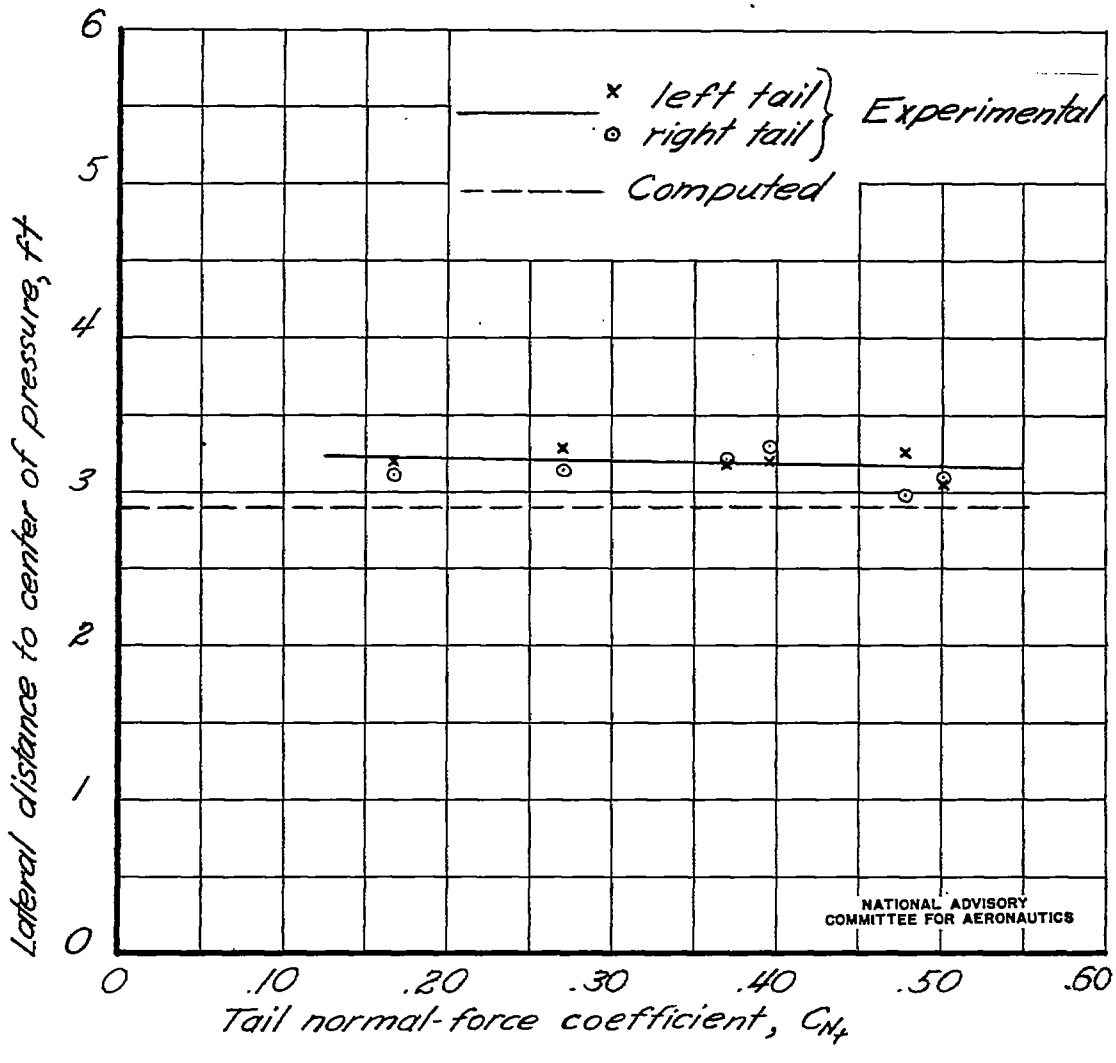

Figure 11. - Variation with tail normal-force coefficient of the measured and computed lateral distance to the center of pressure.